Reflective and Beam –Through Types of Fiber Optic Sensor for Displacement Measurement

WALAA FAWZI AL –MASRI

PHYSICS DEPARTMENT

FACULITY OF SCINCE

UNVERSITY OF MALAYA

KUALA LUMPER

2010

Reflective and Beam –Through Types of Fiber Optic Sensor for Displacement Measurement

By

WALAA FAWZI AL –MASRI

DISSERTATION SUBMITTED TO THE PHYSICS DEPARTMENT, UNVERSITY OF MALAYA IN PARTIAL FULFILLMENT FOR THE MASTER OF TECHNOLOGY MATERIAL SCIENCE

2010

ABSTRACT

This dissertation proposes and demonstrates fiber -optic displacement sensor (FODS) theoretically and experimentally using the intensity modulation technique to measure a displacement from a probe and target. The sensor uses a multimode plastic bundled fiber as a probe and He-Ne laser as a source. The performance of the sensor is compared for different type of probe and target. For a pair type bundled fiber, both the experimental and theoretical results exhibit the same type of characteristic features. The front slope sensitivities are obtained at 1.71 and 1.0 mW/μm for the theoretical and experimental approaches respectively, while the back slope sensitivities are 0.38 and 0.22 mW/μm for the theoretical and experimental approaches respectively, which is smaller than the front slope. By comparing a different type of probe, the result shows that the probe with the largest receiving core diameter demonstrates the highest linearity range, and increasing the number of receiving cores increases the sensitivity of the sensor. With a stainless steel target and the concentric bundled fiber with 16 receiving fibers as a probe, the sensitivity of the sensor is found to be 0.0220 mV/μm over 150 to 550 μm range and -0.0061 mV/μm over 1100 to 2000 μm range. For the beam through type of FODS, only one linear slope is observed. The effect of lateral and axial displacements is investigated. The highest sensitivity is obtained at 0.0008 mV/μm for the lateral displacement. The widest linear range is obtained at 3195mm for the axial displacement.

ACKNOWLEDGEMENT

The writing of this dissertation has been one of the most academic challenging experiences I have ever faced. Without the following people support, patience, and love this dissertation would not be completed. It is to them I would send my deepest gratitude.

- By in large, I want to thank the Al-mighty Allah for my successful life.
- My special thank to my supervisor Mr. Harith Ahmad for his continuous support all trough my dissertation. Moreover to Mr. S.W.Hrun for his patient during I did my dissertation.
- Special thank to Mr. Yasin who was helping me in doing my experiments. His advices and support make my dissertation was complete. He never gives up teaching and supporting me to overcome the obstacles that I faced while doing this dissertation.
- I want to dedicate my dissertation to my parents. To my loving father- I owe you a lot. Your strict discipline has done a lot to shape my life and put me on the right path in this tough life. To my warmhearted mother- I owe you a lot too. Your words of encouragement and push tenacity ring in my ears. I love you both.
- To my brothers I give you my special feelings and gratitude for the memories of laughing, smiling and unconditional love that you give so freely and without compromise. I love you all.

- To my husband Mustafa your sacrifices overwhelmed me. Your encouragement carried me, your special care inspired me and your protection made me feel like I was home.
- To my adorable children Danah and Abdullah- Thank you for letting mommy spend hours and hours studying, reading and writing. Dana, I am sorry I upset you many times. Abdullah, you are my rich gift from Allah for my success. I love you all more than the words of million books.
- To my beautiful friends in Saudi Arabia, Al'anood, Amany, Hawazen, Manal, Lina and Ro'aa- for me, you are not just best friends, but also sisters that I never had. You were there taking away my fears and fulfilling my needs for inspiration to greater levels of success. Your strong commitment in the past two and half years shows you are really friends indeed. I just love being involved with precious friends like you all.

Thank you all for believing in me!

List of Tables:

List of Figures

TABLE OF CONTENTS

CHAPTER 1

INTRODUCTION

1.1 Introduction

Fiber optic sensors are becoming an important subject that attracted many applications in various field s [1, 2]. One of the applications of the sensor is in a high-precision noncontact displacement measurement, which is the key to micro-nano technologies. In a displacement sensor, two methods are commonly adopted, namely laser interferometry and reflective intensity modulation techniques. Laser interferometry [3] which is based on the fringe counting method has high resolution and stability, but its precision and stability is dependent on the wavelength of light. Comparatively, the reflective intensity modulation technique is a significantly simpler method for non-contact displacement measurements while at the same time being able to provide high resolutions. In this type of sensor the reflected light from the mirror is coupled back into a fiber from a reflecting surface and this power is compared to a portion of the power emitted by the same light source. The interest in this type of sensor is based on its inherent simplicity, small size, mobility, wide frequency capability, extremely low displacement detection limit and ability to perform non-contact measurements. These properties have led to a variety of applications, not only as a displacement or vibration sensor, but also as a secondary transducer for measuring physical properties that correlate to the amount of displacement such as temperature [4], pressure [5], and sound [6].

Multimode plastic fibers are in a great demand for the transmission and processing of optical signals in optical fiber communication system. They are also widely used in sensing applications because they provide better signal coupling, have a large core radius and high numerical aperture as well as able to receive the maximum reflected light from the target [7].

In this dissertation, a simple fiber optic displacement sensor is proposed theoretically and experimentally using the intensity modulation technique to measure a displacement from a probe and target. The sensor uses a multimode plastic bundled fiber as a probe and He-Ne laser as a source. This chapter introduces optical fiber and its applications as a sensor. The overview of this dissertation is also described at the end of this chapter.

1.2 History of Fiber Optics

Fiber optics, though used extensively in the modern world, is a fairly simple and old technology. Guiding of light by refraction, the principle that makes fiber optics possible, was first demonstrated by Daniel Colladon and Jacques Babinet in Paris in the early 1840s. John Tyndall included a demonstration of it in his public lectures in London a dozen years later [8-9]. Tyndall also wrote about the property of total internal reflection in an introductory book about the nature of light in 1870. Practical applications, such as close internal illumination during dentistry, appeared early in the twentieth century. Image transmission through tubes was demonstrated independently by the radio experimenter Clarence Hansell and the television pioneer John Logie Baird in the 1920s. The principle was first used for internal medical examinations by Heinrich Lamm in the following decade. In 1952, physicist Narinder Singh Kapany conducted experiments that led to the invention of optical fiber. Modern optical fibers, where the

glass fiber is coated with a transparent cladding to offer a more suitable refractive index, appeared later in the decade [10].

Development then focused on fiber bundles for image transmission. The first fiber optic semi-flexible gastroscope was patented by Basil Hirschowitz, C. Wilbur Peters, and Lawrence E. Curtiss, researchers at the University of Michigan, in 1956. In the process of developing the gastroscope, Curtiss produced the first glass-clad fibers; previous optical fibers had relied on air or impractical oils and waxes as the low-index cladding material. A variety of other image transmission applications soon followed. Jun-ichi Nishizawa, a Japanese scientist at Tohoku University, was the first to propose the use of optical fibers for communications in 1963 [11]. Nishizawa invented other technologies that contributed to the development of optical fiber communications as well. Nishizawa invented the graded-index optical fiber in 1964 as a channel for transmitting light from semiconductor lasers over long distances with low loss [9].

In 1965, Charles K. Kao and George A. Hockham of the British company Standard Telephones and Cables (STC) were the first to promote the idea that the attenuation in optical fibers could be reduced below 20 decibels per kilometer (dB/km), allowing fibers to be a practical medium for communication [9]. They proposed that the attenuation in fibers available at the time was caused by impurities, which could be removed, rather than fundamental physical effects such as scattering. The crucial attenuation level of 20 dB/km was first achieved in 1970, by researchers Robert D. Maurer, Donald Keck, Peter C. Schultz, and Frank Zimar working for American glass maker Corning Glass Works, now Corning Incorporated. They demonstrated a fiber with 17 dB/km attenuation by doping silica glass with titanium. A few years later they produced a fiber with only 4 dB/km attenuation using germanium dioxide as the core

dopant. Such low attenuations ushered in optical fiber telecommunications and enabled the Internet. In 1981, General Electric produced fused quartz ingots that could be drawn into fiber optic strands 25 miles (40 km) long.

Attenuations in modern optical cables are far less than those in electrical copper cables, leading to long-haul fiber connections with repeater distances of 70–150 kilometers (43–93 mi). The erbium-doped fiber amplifier, which reduced the cost of long-distance fiber systems by reducing or even in many cases eliminating the need for optical-electrical-optical repeaters, was co-developed by teams led by David N. Payne of the University of Southampton, and Emmanuel Desurvire at Bell Laboratories in 1986 [12-13]. The more robust optical fiber commonly used today utilizes glass for both core and sheath and is therefore less prone to aging processes. It was invented by Gerhard Bernsee in 1973 of Schott Glass in Germany.

In 1991, the emerging field of photonic crystals led to the development of photonic-crystal fiber [14] which guides light by means of diffraction from a periodic structure, rather than total internal reflection. The first photonic crystal fibers became commercially available in 2000. Photonic crystal fibers can be designed to carry higher power than conventional fiber, and their wavelength dependent properties can be manipulated to improve their performance in certain applications.

1.3 Fiber Optic Sensor Technology

Optical fiber are long, thin strands of very pure glass about the diameter of a human hair. They are arranged in bundles called optical cables and used to transmit light signals over long distances. A bare fiber consists of three parts: core, cladding and

buffer coating or jacket. The core is a thin glass or plastic center of the fiber where the light travels while the cladding is an outer optical material surrounding the core that reflects the light back into the core. Buffer coating is a plastic coating that protects the fiber from damage and moisture. Fiber optic technology offers the possibility for developing of a variety of physical sensor for a wide range of physical parameter. The use of optical fiber as the sensor probe allows in obtaining a very high performance in their response to many physical parameters (displacement, pressure, temperature, electric field) compared to conventional transducer [15]. Almost thirty years have passed since the study of optical fiber sensors began. Various ideas have been proposed and various techniques have been developed for various measured and applications. To date, some types of optical fiber sensors have been commercialized but it is also true that, among the various techniques that have been studied, only a limited number of techniques and applications have been commercially successful [16].

Optical fiber sensors have advantages such as dielectric construction, giving electrical isolation [17], immunity to electromagnetic interference (EMI), lightweight, small size, easy in signal light transmission, large bandwidth, compactness, geometric versatility and economy. In general, FOS is characterized by high sensitivity when compared to other type of sensor. It is also passive in nature due to the dielectric construction. Specially prepared fibers can withstand high temperature and other harsh environments. In telemetry and remote sensing application it is possible to use a segment of fiber as a sensor gauge while a long length of the same or another fiber can convey the sensed information to a remote station. In many fields of application, optical fiber sensors should compete with other rather mature technologies such as electronic measurements.

There are varieties of fiber optic sensors, which can be classified according to the detection techniques such as intensity (amplitude), phase, frequency, or polarization sensor. Since detection of phase or frequency in optics is also referred to interferometric technique, this sensor is also termed as an interferometric sensor. Fiber optic sensor can also be classified on the basis of their applications: physical (e.g. measurement of temperature, stress, etc.); chemical sensor (e.g. measurement of pH content, gas analysis, spectroscopic studies, etc.); biomedical sensors (inserted via catheters or endoscopes which measure blood flow, glucose content and so on). Both the intensity types and the interferometric types of can be considered in any of the above applications [18]. Another classification of optical fiber depending on how they work and this type of sensors are classified as extrinsic or intrinsic sensor.

1.4 Application of Fiber Optic Sensor

Fiber optic sensor have been subject to considerable research for the past 30 years or so since they were first demonstrated about 40 years ago [19]. These new sensing technologies have formed an entirely new generation of sensor offering many important opportunities and great potential for diverse applications. The most highlighted application fields of FOS are in large composite and concrete structures, the electrical power industry, medicine, chemical sensing, and the gas and oil industry. Fiber optic sensor have several distinguishing advantages in comparison with traditional electrical sensor like potential capability of surviving in harsh environments, A much less intrusive size for embedding into composites without introducing any significant perturbation of the structure, Greater resistance to corrosion when used in open structures, such as bridges and dams. These features have made them very attractive for quality control during construction, health monitoring after building, impact monitoring

of large composite or concrete structures. Some applications of these sensor in bridges, dams, mines, and aircraft have been demonstrated [20].

1.5 Overview of This Dissertation

Chapter 1 describes the background of the fiber-optic sensor technology as well as a basic concept of the fiber-optic sensors. The history of fiber-optic is also discussed in this chapter.

Chapter 2 presents a literature review on the fiber optic displacement sensor which is based on intensity modulation technique. The theoretical analysis of optical fiber displacement sensor is also carried out using a Gaussian beam approach. The working principle of pair and concentric types of fiber optic displacement sensor is also described in terms of stability, sensitivity and resolution.

Chapter 3 demonstrates reflection types of FODS experimentally .The experimental results are compared with the theoretical results obtained from the analysis in chapter 2.

Chapter 4 describes the lateral and axial displacement experiment using fiber optic sensor based on beam through technique. This dissertation is concluded in

Chapter 5

CHAPTER 2

LITERATURE REVIEW AND THEORETICAL BACKGROUND

2.1 Introduction

This chapter reviews on fiber-optic technology and its application in sensor. The basic principle of fiber-optic is described and the fiber-optic sensor is thoroughly reviewed in this chapter. Then the fiber-optic displacement sensor (FODS) is introduced and explained. At the end of this chapter, the theoretical background of the FODS is also described.

2.2 Review On The Fiber-Optic Technology

2.2.1 Introduction to Fiber-Optic

An optical fiber (or fibre) is a glass or plastic fiber that carries light along its length. Fiber optics is the overlap of applied science and engineering concerned with the design and application of optical fibers. Optical fibers are widely used in fiber-optic communications, which permits transmission over longer distances and at higher bandwidths (data rates) than other forms of communications. Fibers are used instead of metal wires because signals travel along them with less loss, and they are also immune to electromagnetic interference. Fibers are also used for illumination, and are wrapped

in bundles so they can be used to carry images, thus allowing viewing in tight spaces. Specially designed fibers are used for a variety of other applications, including sensors and fiber lasers.

Light is kept in the core of the optical fiber by total internal reflection. This causes the fiber to act as a waveguide. Fibers which support many propagation paths or transverse modes are called multi-mode fibers (MMF), while those which can only support a single mode are called single-mode fibers (SMF). Multi-mode fibers generally have a larger core diameter, and are used for short-distance communication links and for applications where high power must be transmitted. Single-mode fibers are used for most communication links longer than 550 meters. FODS normally uses multimode fiber as a probe.

2.2.2 Optical Fiber Material

Optical fibers are fabricated from glass or plastic or sometimes both of them. Plastic fibers have a major drawback i.e. a relatively high loss of light transmission and it could use for short length of transmission. However, this kind of fiber provides a relative easy termination of the fiber ends. On the other hands, glass fiber have a relatively low loss and can be exploited over long distances of transmission, however the termination of the fiber end is more difficult and sometimes create problems. Careful attention to polishing and controlling the cutting method will take care of this drawback. In addition, plastic optical fibers (POFs) can operate successfully at wavelengths 650 nm while the 850-nm and 1300-nm laser diodes used with glass optical fibers (GOFs). Some general benefits of POFs are the simpler and less expensive components, lighter weight, operation in the visible wavelength range, greater

flexibility, immunity to EMI, ease in handling and connecting, and greater safety than GOF. With these advantages one most consider the following disadvantages: High-loss, a lack of system provider, a lack of standards, and limited production. However, the high-loss problem is being addressed with the new per fluorinated polymer materials, which have brought losses down to potentially 10dB/km [21]. Since POFs have larger core diameters (about 1 mm) than glass fibers (8–100μm), their connectors are less cost less, and are less likely to suffer damage than connectors for glass fibers. Thus such connector can be made from plastic rather than the precision-machined stainless steel or ceramics that GOF requires.

Because of the ease of coupling light from light source, it is possible to embed the source and drive electronics into the connector housing, such as for transceivers used in automotive and consumer products [22]. Finally, because of ease of coupling the POF to a photo detector, the required connector can be made from plastic and at a lower cost. Design and performance of a plastic optical fiber as a probe for the fiber-optic sensors are reported recently [23].

In order to optimize the performance of the fiber, several mixture have been selected to give better strength, lower attenuation ,better flexibility, or specific parameter requirements. The mixtures of oxides, sulfides, or selenides are the most common ingredients in producing a high quality optical fiber [24]. The optical fiber is coated by the polymer after drawing process to improve the strength of the fiber. Coating can be also a significant factor in the reduction of micro-bending losses.

2.2.3 Type of Fibers

There are several type of fibers used commercially in the areas of communication, medical imaging and sensors. They made differently, operate in different ways. Low attenuation fiber is required to maximize spacing of repeaters or amplifiers in transmission link. In optical communication applications, the transmission fiber has a loss as low as 0.16 dB/km at 1550nm. Nowadays, there are two most common operating classes of fiber based on their modal properties utilized in sensor technology; single-mode fibers and multimode fibers. Single-mode fibers are classified into three different types of fiber i.e step-index, dispersion–shifted and dispersion–flattened. On the other hand, multimode fibers are grouped into two types; step-index and graded–index fibers

Single mode fibers (SMFs) are mostly available with step-index profile [22]. The step index fiber has a higher index of refraction for the core compared to the cladding, which resulted in total internal reflection at the core cladding interface. The peak difference in refractive indices of the core and cladding is estimated around 1 to 20% in this fiber. The index difference determines the numerical aperture of the fiber, which in turn determines the amount of light the fiber can be collected from an optical source. The SMF usually has a very small core dimeter (5-10μm) and allows only one mode to propagate effectively in the core as shown in Fig. 2.1. The primary advantages of SMF is that the multimode dispersion is eleminated since only one mode is being propagated in the core.

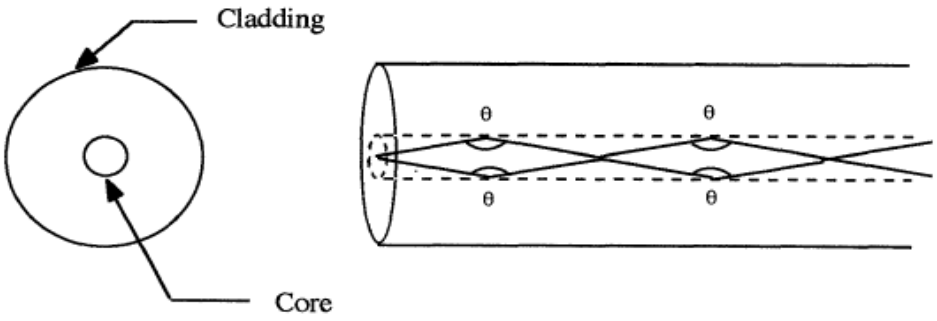

Fig. 2.1: Transmission modes of light in the step-index single-mode core where the light is reflected with the same pattern of angle from wall to wall.

Another type of SMF is dispersion-shifted fiber (DSF), which is invented to reduce the chromatic dispersion. This fiber has two layers of core and cladding with the inner core has a refractive index graded with triangular profile which is surrounded by an inner cladding. The next layer is the outer core layer which refractive –index is higher than the inner cladding but lower compared to inner core and this layer too is wrapped with an outer cladding. This index structure has shifted the point of zero dispersion from 1300nm to 1550 nm where attenuation is considerably lower. The main advantage by shifting the zero dispersion is that repeater spacing could be stretched as far as 80km range. However, the shifting has increased the fiber attenuation slightly above that of step-index SMFs and could only be operated at 1550 nm. Fig. 2.2 compares the typical cross-section and refractive index profile for both step index SMF and DSF.

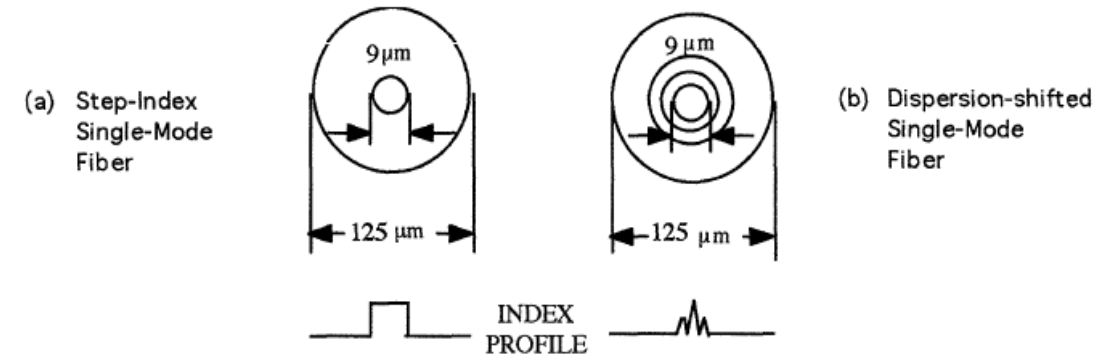

Fig. 2.2: (a) the cross-section of the step-index SMF where the glass composition changes abruptly (b) the cross-section of the dispertion-shifted single-mode fiber with inner and outer layer change the refractive index profile of the fiber.

Multimode fibers could be classified into step-index and graded-index multimode fibers. The term multimode means that light can be propagated in the same wavelength along different ways through a fiber which causes the waves to arrive at the opposite end of fiber at different time. This fiber is not suitable for optical communication but is very useful in sensor applications. The major attraction of step-index multimode fibers is easy for collecting light because of larger core size compared to SMF. Typical numerical apertures (NA) of this fiber ranges from 0.2 to 0.4 and their core diameter usually ranges from 100 μm to 200 μm. The combination of large core diameter and high numerical apertures allows the use of inexpensive large-area light sources such as LED and avoids the precise connecors problem.

With the rapid advancement of technology in optical fiber, a new type of MMFs so-called graded –index multimode fiber is invented. The fiber could deal with drawback of step-index multimode, especially in reducing the high model dispersion. The term “graded “conveys the meaning of fiber having a “gradually” change of refractive–index profile from core to cladding causes light rays to bend back toward the

axis as they propagate, thus minimize the difference in time that light rays take to pass through the fiber. Graded–index MMFs have smaller dimension in both core and cladding compare to step-index multimode. The core diameter typically ranges from 50 µm to 85 µm and the cladding diameter is usually around 100 µm. The graded-index multimode has a core diameter large enough compared to step-index single mode which result an ease of coupling tolerance but still carry many modes. Fig. 2.3 shows the cross section of both step index and graded index MMFs. Fig. 2.4 shows the light propagation in both step index and graded index MMFs. As shown in Fig. 2.4, the light propagation of step-index MMF is described as zigzag path between core-cladding boundaries on each side of fiber axis. However, the graded refractive –index bends the light beams back toward the axis to reduce the multimode dispersion effect.

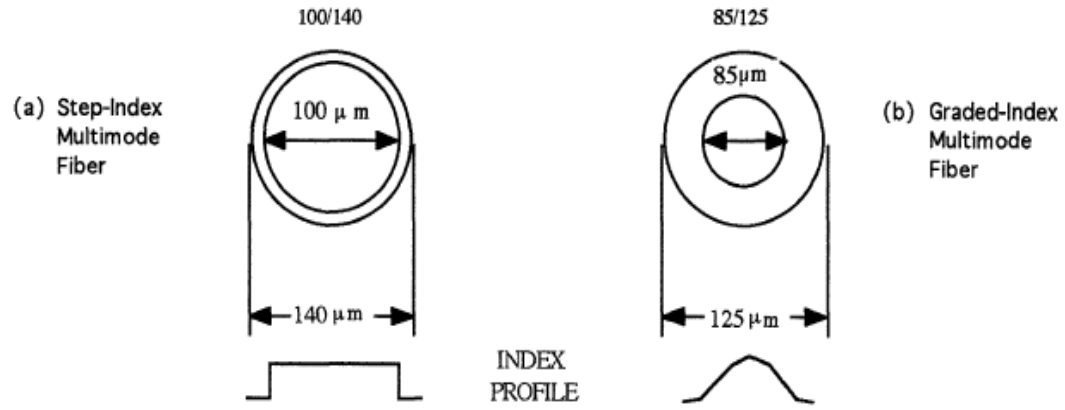

Fig. 2.3. Typical multimode fiber cross-section (a) the cross-section of step-index multimode fiber with an abrupt refractive index (b) the cross-section of graded-index multimode fiber with gradually changes from core to cladding of refractive index profile.

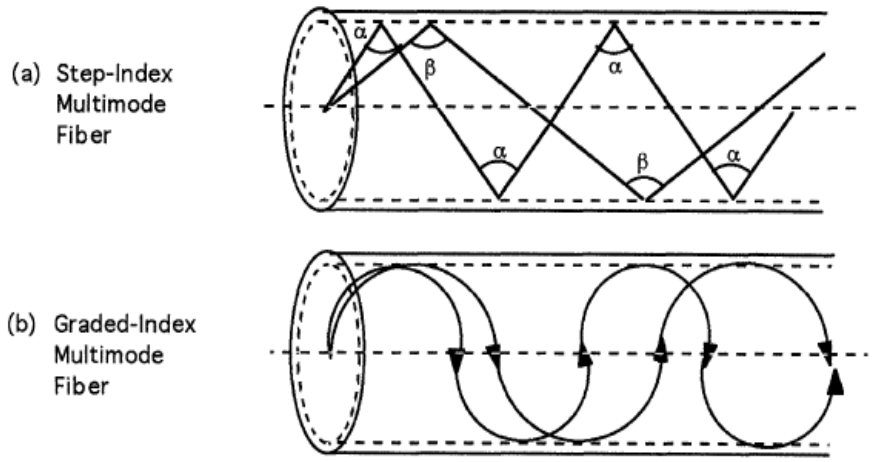

Fig. 2.4: Typical light propagation inside the MMFs (a) step-index multimode fiber (b) graded–index multimode fiber

2.2.4 Operation Principle of Optical Fiber

Light is kept in the core of the optical fiber by total internal reflection that occurs when a ray of light strikes a medium boundary at an angle larger than the critical angle with respect to the normal to the surface. If the refractive index is lower on the other side of the boundary no light can pass through, so effectively all of the light is reflected. The critical angle is the angle of incidence above which the total internal reflection occurs. When light crosses a boundary between materials with different refractive indices, the light beam will be partially refracted at the boundary surface, and partially reflected. However, if the angle of incidence is greater (i.e. the ray is closer to being parallel to the boundary) than the critical angle--the angle of incidence at which light is refracted such that it travels along the boundary--then the light will stop crossing the boundary altogether and instead totally reflect back internally. This can only occur where light travels from a medium with a higher refractive index to one with a lower

refractive index. For example, it will occur when passing from glass to air, but not when passing from air to glass.

Fig. 2.5 describes the total internal reflection phenomena in step index optical fiber. As shown in the figure, the light that enters with an angle less than cone half angle will be reflected throughout the cladding walls while the light that enters with an angle large than cone half angle will eventually loss by radiation. The core half-angle or sometimes it is called as the acceptance angle is defined as the maximum angle which the light will be reflected when entering the media otherwise it will be lost by radiation . The reflection of light is made possible by higher refractive index of the core and a lower refractive index of the cladding since light will be totally reflected when it strikes a boundary with a material of lower refractive index at a large incident angle.

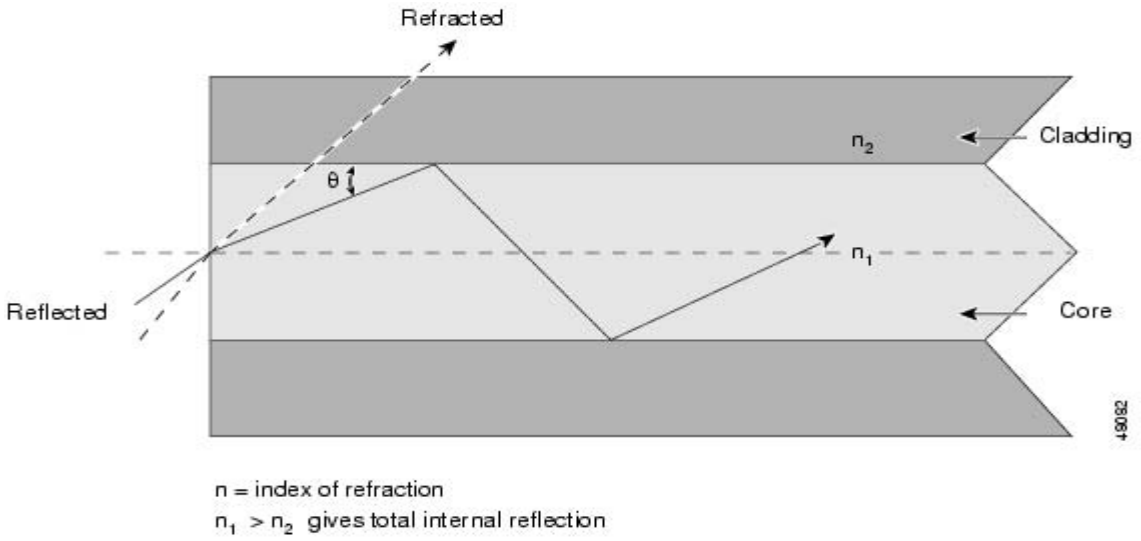

Fig. 2.5: Total Internal Reflection

2.2.5 Numerical Aperture

Numerical aperture is another property to explain a light propagation in optical fiber. It is defined as the sine of acceptance angle as described in Fig. 2.6. Numerical aperture determines the ability of the optical fiber to collect the incident light and how it spreads out after leaving the fiber. Numerical aperture or NA depends on core refractive index, cladding refractive index and half acceptance angle and is given by;

$$NA = n \sin \theta_{\max} = \sqrt{n_f^{\,2} - n_c^{\,2}} \qquad \text{(Eq. 2.1)}$$

Where n is the refractive index of the medium outside the fiber (air), n_f is the refractive index of the fiber core and n_c is the refractive index of the cladding. θ_{max} is the half acceptance angle described in Fig. 2.6.

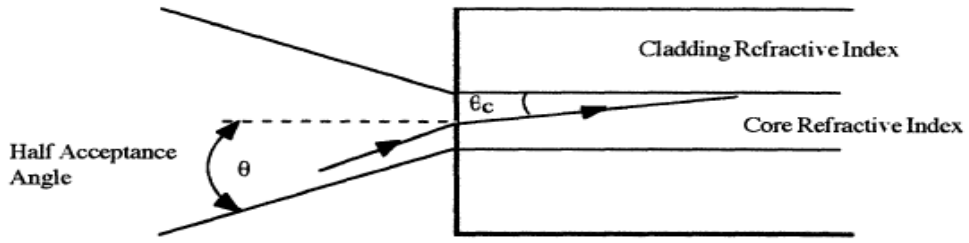

Fig. 2.6: Acceptance angle

2.2.6 Plastic Fibers

Plastic fiber-optic cable usually consists of a single strand typically 0.254–1.52 mm diamter. These fibers are flexible, and excellent for applications that require repeated flexing as well as for use in extremely tight areas. They generally are sold with a cutting device that allows customers to trim to the desired length. In recent years, many companies have released multi-core high-flex plastic fiber or bundled fibers. These differ from conventional plastic fibers in having multiple independent cores, a

configuration that allows a bending radius as small as 1 mm and thus flexibility close to that of electric wire. They can be bent at 90° with no reduction of light transmission, and readily conform to machine contours without the problems associated with extreme vibrations or pulling. Various vendors also offer coiled versions of plastic fibers for applications that require articulated or reciprocating motions. When the sensor will be exposed to harsh chemicals, solvents, or high temperatures, glass fibers are preferable. But plastic fibers can be sheathed with Teflon, nylon, or polypropylene for added immunity to hostile environments.

In this dissertation, various fiber-optic displacement sensors are demonstrated using the bundled plastic fibers. The fiber-optic displacement sensor will be introduced in the section.

2.3 Fiber-Optic Sensors for Displacement Measurements

Over the past twenty years, the tremendous growth of the optoelectronics and fiber optic communications industries has taken place. This industry has literally revolutionized the telecommunication industry by providing higher performance, more reliable telecommunication links with ever decreasing bandwidth cost. This revolution is bringing about the benefits of high volume production to component users and a true information superhighway built of optical fiber. In parallel with these developments, fiber optic sensor [25-29] technology has been a major user of technology associated with the optoelectronic and fiber optic communication industry. Many of the components associated with these industries were often developed for fiber optic sensor applications.

Fiber optic sensor technology in turn has often been driven by the development and subsequent mass production of components to support these industries.

As component prices have fallen and quality improvements have been made, the ability of fiber optic sensors to displace traditional sensors for rotation, acceleration, electric and magnetic field measurement, temperature, pressure, acoustics, vibration, linear and angular position, strain, humidity, viscosity, chemical measurements and a host of other sensor applications, has been enhanced. In the early days of fiber optic sensor technology most commercially successful fiber optic sensors were squarely targeted at markets where existing sensor technology was marginal or in many cases nonexistent. The inherent advantages of fiber optic sensors which include their ability to be lightweight, of very small size, passive, low power, resistant to electromagnetic interference, high sensitivity, wide bandwidth and environmental ruggedness were heavily used to offset their major disadvantages of high cost and unfamiliarity to the end user.

A bifurcated optical fiber bundle based sensors presented in this dissertation can have many applications. Having high sensitivity to short distances, bifurcated optical fiber bundles are well suited not only for control applications as position sensors, but also for gauging and surface assessment [30], [31]. In addition, they can be utilized as noncontact pressure sensors if used in conjunction with reflective diaphragms moving in response to pressure [30]. Bifurcated optical fiber bundles can also be applied as temperature transducers if used in conjunction with deformable bimetal sensors [32]. Fig. 2.7 depicts the basic setup of a typical multimode intensity sensor using lower technology fiber bundles for displacement measurement purposes. It consists of an optical source (e.g., laser), a photo detector, an optical power meter, a branched fiber bundle, and a planar mirror. The amount of light returning to the detector depends on the distance between the end of the bundle and the mirroring surface being monitored

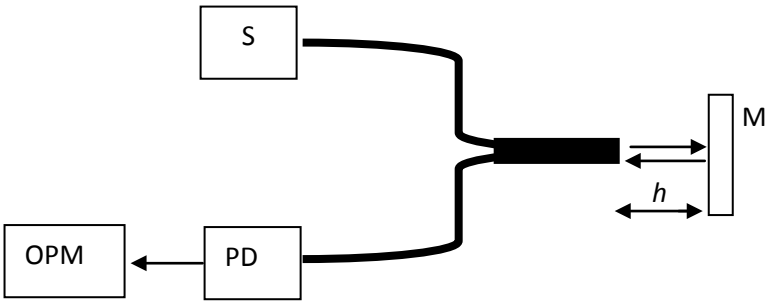

Fig. 2.7: Basic configuration of a bifurcated fiber bundled displacement sensor.

2.4 Light Source for Fiber-Optic Displacement Sensors

The rapid progress in the field of optical communication and sensors has been made possible by the development of low–loss optical fiber and light source that are compatible with the spectral transmission characteristics and physical dimensions of these fibers. A helium-neon laser usually called a HeNe laser is normally used for fiber-optic displacement sensor system. It is a small gas laser of a type and also often used in laboratory demonstrations of optics. Its usual operation wavelength is 632.8 nm, in the red portion of the visible spectrum or sometimes 543nm (green) and 594nm (yellow). The gain medium of the laser, as suggested by its name, is a mixture of helium and neon gases, approximately in the ratio 5:1, contained at low pressure (typically ~300 Pa) in a glass envelope. The energy or pump source of the laser is provided by an electrical discharge of around 1000 V through an anode and cathode at each end of the glass tube. The cavity of the laser typically consists of a plane, high-reflecting mirror at one end of the laser tube, and a concave output coupler mirror of approximately 1% transmission at the other end. HeNe lasers are typically small, with cavity lengths of around 15 cm up to 0.5 m, and optical output powers ranging from 1 mW to 100 mW.

The laser process in a HeNe laser starts with collision of electrons from the electrical discharge with the helium atoms in the gas. This excites helium from the ground state to the 2^3S_1 and 2^1S_0 long-lived, metastable excited states. Collision of the excited helium atoms with the ground-state neon atoms results in transfer of energy to the neon atoms, exciting them into the 2s and 3s states. This is due to a coincidence of energy levels between the helium and neon atoms. This process is given by the following reaction equation:

$$He^* + Ne \rightarrow He + Ne^* + \Delta E \qquad \text{(Eq. 2.2)}$$

where (*) represents an excited state, and ΔE is the small energy difference between the energy states of the two atoms, of the order of 0.05 eV.

The number of neon atoms entering the excited states builds up as further collisions between helium and neon atoms occur, causing a population inversion between the neon 3s and 2s, and 3p and 2p states. Spontaneous emission between the 3s and 2p states results in emission of 632.8 nm wavelength light, the typical operating wavelength of a HeNe laser. After this, fast radiative decay occurs from the 2p to the 1s energy levels, which then decay to the ground state via collisions of the neon atoms with the container walls. Because of this last required step, the bore size of the laser cannot be made very large and the HeNe laser is limited in size and power. With the correct selection of cavity mirrors, other wavelengths of laser emission of the HeNe laser are possible. The 3s→3p and 2s→2p transitions give infrared operation at 3.39 μm and 1.15 μm wavelengths, and a variety of 2s→1s transitions are possible in the green (543.5 nm, the so-called Green He-Ne laser), the yellow (594 nm) and the orange (612 nm).

The gain bandwidth of the laser is dominated by Doppler broadening, and is quite narrow at around 1.5 GHz. This, along with the visible output and excellent beam quality possible from these lasers, makes the HeNe a useful source for holography and as a reference for spectroscopy. Other applications include use in barcode scanners

Another alternative light source for the sensor is light emitting diode (LED). Some of feature of light –emitting diode that are of interest of fiber optic sensor include a longer life span, a very long coherence length, greater stability, wider temperature range, very low sensitivity to break reflection from elements of the fiber optic sensor since emission is dominated by spontaneous emission, and relativity inexpensive compared to conventional light source. LED consists of material such as gallium arsenide phosphide (GaAsP) and therefore its effectiveness absolutely depends on the emitted wavelength where the shorter wavelength the less efficient the LED becomes. The characteristic which generally considered when selecting an LED as a light source for fiber optic system are: wavelength, spectral width, power, coupling, and current – voltage characteristic, some LED could perform in the range of 800 nm to 1400nm.

2.5 Optical Detector for Fiber Optic Displacement Sensor

Optical detector is an important component in any fiber optic system like the optic fiber or the light source. The detector operates by converting the received luminous flux of photons into electron by an electronic system such as a reverse biased semiconductor PIN photodiode. Fig. 2.8 shows the working principle of optical detector. In the detector, electron hole carrier pairs are separated by the high electrical field in depletion region as the incoming photons are absorbed. As the carriers traverse the depletion zone, the displacement current is induced at the load as the signal current.

The detector receives signals from light source through optical fiber thus convert them into electrical current.

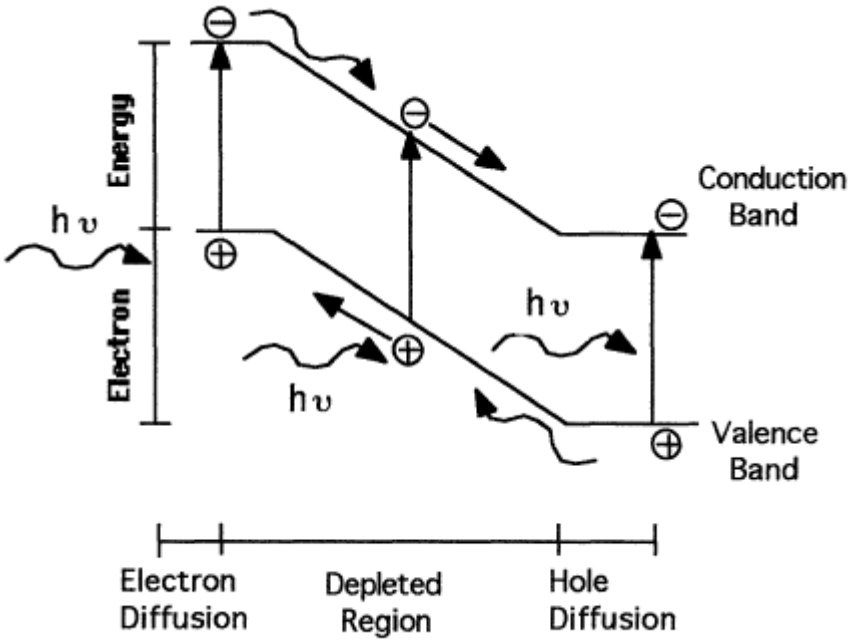

.

Fig. 2.8: absorption of photon in photo detector

Two type of detector are used widely in fiber optic industry: semiconductor photodiode (PD) and avalanche photodiode (APD). Both of them exhibit fast rise time and acceptable bandwidth parameter. APD is more expensive and required an auxiliary power supply but it provides receiver sensitivity as well as signal amplification without sacrificing high –speed operation.

2.6 Sensor Performance Parameters

There are some parameter used to show the performance of optical fiber sensor such as stability and drift, sensitivity, resolution and linear range. The stability expresses the capacity to maintain the system characteristics with time and, specifically,

the transfer curve. The drift indicates the variation of the system characteristics in a non-recoverable and therefore permanent way, whatever its causes (environmental conditions, function, or even their storage). There are two problems regarding the transfer function, drift from zero or offset drift (an output appears with zero input), or drift from the slope (and therefore the sensitivity), or combinations of both. Given a working point of the sensor, the drift can be expressed quantitatively through measurements at the output, as the absolute variation of the output relative to the ideal output value that should be delivered.

$$\text{Drift} = [\Delta V/(V_1)] \times 100 \quad \text{(in \%)} \qquad \text{(Eq. 2.3)}$$

The point and the conditions of operation of the sensor, and the lapse time of the measurement should also be expressed.

Conceptually and in general, sensitivity expresses the reaction capacity of the system to the input stimulus. It is a characteristic of the dynamic function (notations of the variables in lower case). For this reason, quantitatively, the sensitivity is expressed by the calibration curve pre-determined by the constant value of the desired input variable. Thus, in general, the value depends on the working point of the calibration curve at which the measurement is to be made. In other words, the Absolute Sensitivity can be expressed:

$$S_\alpha = \Delta V/\text{slope} \qquad \text{(Eq. 2.4)}$$

Resolution is the minimum input variation which can be detected and measured in the sensor with minimum quality. Measurement range is defined as the range of values of the input of the varible (max displacment – min displacement)

2.7 Theoretical Model of Bundled Fiber

The basic set-up for a displacement sensor consists of a modulated light source, a detector and a Y branched bundled fiber and a planar mirror. The Y branched bundled fiber consists of a pair and a concentric of transmitting and receiving fibers as shown in Figure 2.9 (a) for the pair and (b) for the concentric bundled fiber. Displacement is measured by comparing the power of the reflected light, which is coupled back into a receiving fiber from a mirror, with a portion of power emitted by the same light source. The amount of light that returns to the detector depends on the distance between the end of the bundled fiber and the mirroring surface being monitored. In order to analyze the displacement sensing characteristic theoretically, the following assumptions are made [32]:

(a) The pair bundled fiber in front of the mirror is modeled as a set of two independent parallel equal fibers in contact with each other with no space left between them. Both the transmitting and receiving fibers are assumed to have perfectly circular cross sections with area S_a and radius w_a as shown in Figure 2.9 (a) and the concentric bundled fiber with areas of S_a and S_b and radii of w_a and w_b, respectively as shown in Figure 2.9 (b).

(b) The light leaving the transmitting fiber is represented by a perfectly symmetrical cone with divergence angle θ_a, and vertex 0 located at a distance z_a inside the fiber, as shown in Figure 2.9 (a) and (b).

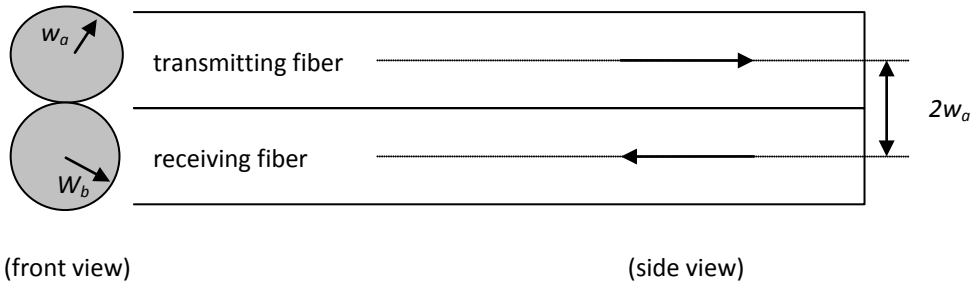

(a)

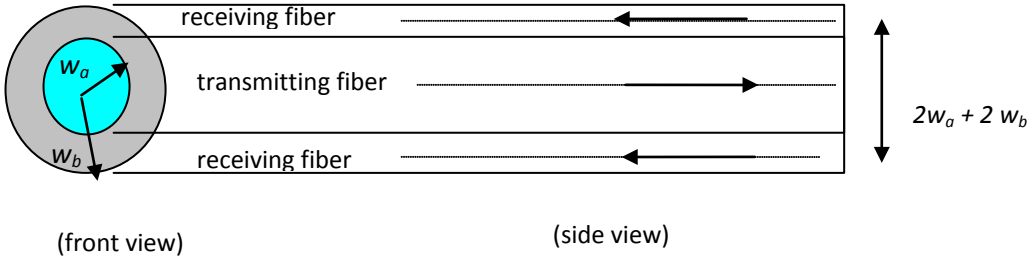

(b)

Fig. 2.9: Front and side views of the transmitting and receiving bundled fiber ends (a) for the pair and (b) for the concentric bundled fiber.

In order to evaluate the amount of light collected by the receiving fiber, the light cone is extended beyond the mirror as shown in Fig 2.10 (a) for the pair and (b) for the concentric bundled fiber and the image position at the receiving end is analyzed. A z-coordinate is introduced which is aligned to the emitted light cone axis beginning at 0 and extending beyond the mirroring surface. M the coordinate of the center point in the receiving fiber end is designated as Q′ as shown in Figure 2.10 (a) and (b) for bundled fiber with type A,B, and C, respectively are represented by:

$$\text{Q}' \begin{cases} y = 2w_a \\ z = z_a + 2h \end{cases} \qquad \text{Q}' \begin{cases} y = \frac{3}{2} w_a \\ z = z_a + 2h \end{cases} \qquad \text{Q}' \begin{cases} y = \frac{5}{4} w_a \\ z = z_a + 2h \end{cases} \qquad \text{(Eq. 2.5)}$$

where *h* is the distance being monitored and $w_a = w_b$ (type A), $w_a = 2w_b$ (type B) and $w_a = 4w_b$ (type C).

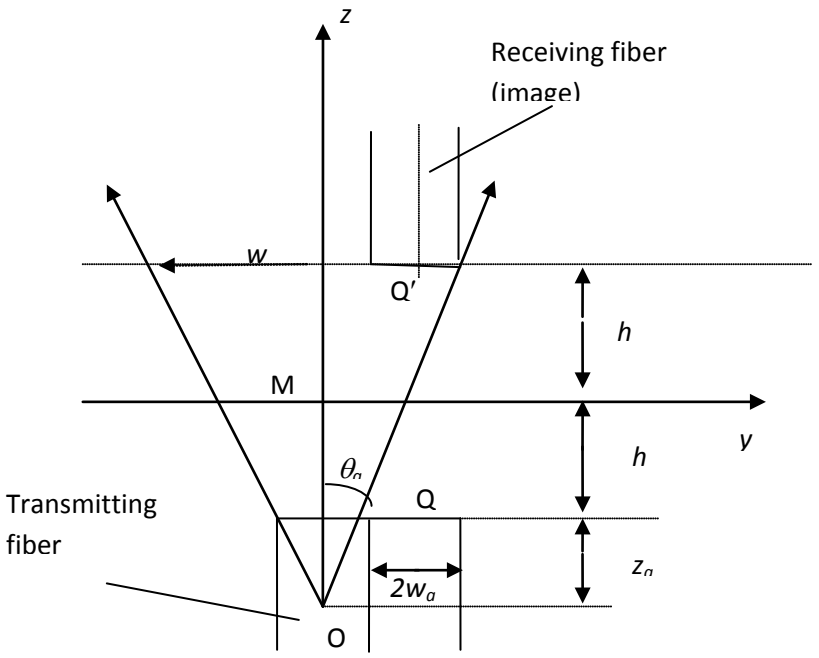

(a) type A

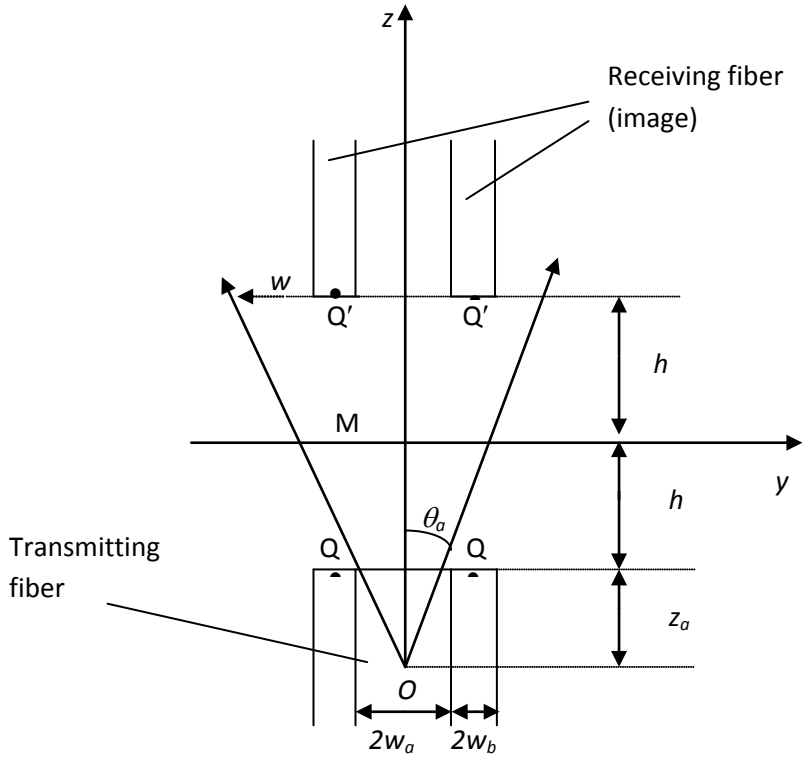

(b) Type B and type C.

Fig. 2.10: Cone of light exiting the transmitting fiber, the cone is extended beyond the mirror and the image position of the receiving end (a) for type A and (b) for type B and type C.

The theoretical approach is based on the electromagnetic theory of paraxial Gaussian beams, which is used to derive the transfer function that is dependent on the variance of the optical power collected by the receiving fiber bundle. This approach describes the light leaving the transmitting fiber bundle as a paraxial beam with a Gaussian profile. The irradiance of the emitted light decreases rapidly over the beam cross-sections, obeying an exponential law according to

$$I(r,z) = \frac{2P_E}{\pi w^2(z)} \exp\left(-\frac{2r^2}{w^2(z)}\right) \qquad \text{(Eq. 2.6)}$$

where r is the radial coordinate, z is the longitudinal coordinate and radius $w(z) = w_0\sqrt{1+(z/z_R)^2}$ is a measure of the beam width whose dependence is on z . The constants w_0 and z_R are the waist radius and Rayleigh range respectively and their relationship is given by;

$$\pi w_0^{\,2} = \lambda z_R \qquad \text{(Eq. 2.7)}$$

In the case of the points situated in the far-field zone ($z >> z_R$), the beam resembles a spherical wave confined within a cone as depicted in Figure 2.10. The cone is characterized by a divergence angle given by:

$$\theta_a \approx \tan\theta_a = \frac{w(z)}{z} = \frac{w_0}{z_R} = \frac{\lambda}{\pi w_0} \qquad \text{(Eq. 2.8)}$$

and the irradiance function can be simplified as:

$$I(r,z) = \frac{2P_E}{z^2\pi\theta_a^{\,2}}\exp\left(-\frac{2r^2}{\theta_a^{\,2}z^2}\right) \qquad \text{(Eq. 2.9)}$$

The optical power collected by the receiving fiber is evaluated by integrating *I(r,z)* over the fiber end surface S_a as shown below:

$$P(z) = \int_{Sb} I(r,z)dS\,. \qquad \text{(Eq. 2.10)}$$

We assume that the irradiance *I(r,z)* is approximately constant across the receiving surface with area $S_a = \pi w_a^{\,2}$, and equal to its value at the canter of the receiving fiber (point Q′) where $r = 2w_a \approx 2\theta_a z_a$ (for the pair bundled fiber) . In this case, we obtain

$$P = IS_b = \frac{2P_E}{\zeta^2}\exp\left(-\frac{8}{\zeta^2}\right) \qquad \text{(Eq. 2.11)}$$

where

$$\zeta = \frac{z}{z_a} = 1 + \frac{2h}{z_a} = 1 + 2h_N \qquad \text{(Eq. 2.12)}$$

and h_N is a relative displacement. By analyzing $dP/d\zeta = 0$, the collected power reaches its maximum value $P_{\max} = [(P_E/4)\exp^{-1}]$ when $\zeta = \sqrt{8}$ (i.e., $h_N = 0.9142$). Taking this into account, we may rewrite (Eq. 2.11) in normalized form $P_N = P/P_{\max}$ as

$$P_N = \frac{8}{\zeta^2}\exp\left(1 - \frac{8}{\zeta^2}\right) \qquad \text{(Eq. 2.13)}$$

A relative displacement can be evaluated using Eq. 2.13. And Fig. 2.10. If, r = 0.5mm, λ = 633nm and w_0 = 0.46mm, z_a is calculated to be 1141mm. By using $h_N = h/z_a$, we obtain $h_N = [(h/1141)x10^{-3}]$ in arb, Units, where h is a displacement, which has moved in 50μm steps in the experiment. For the portion of a linear curve, the sensor sensitivity is evaluated by deriving of P_N with respect to h_N

$$S = \frac{\partial P_N}{\partial h_N} \qquad \text{(Eq. 2.14)}$$

Making use of Eq. 2.13, we get:

$$S = 2\frac{\partial}{\partial \zeta}P_N = \frac{4}{\zeta}\left(\frac{8}{\zeta^2} - 1\right)P_N(\zeta) \qquad \text{(Eq. 2.15)}$$

The performance of the optical fiber displacement sensor for a pair and concentric types of bundled fiber probe are calculated using both Eqs. (2.13) and (2.15). Table 2.1 summarizes the characteristic of the fibers bundled used in our experiment. The

theoretical results will be presented and compared with the experimental results in next chapter.

Table 2.1: Fiber bundled probe used in the experiment

	Type	No. of core inside the receiving fiber	Transmitting fiber's diameter	Receiving fiber's diameter	Arrangement of fiber in the bundle
1	Type A	1	1.00 mm	1.00 mm	Pair
2	Type B	9	0.50 mm	0.25mm	Concentric
3	Type C	16	1.00mm	0.25mm	Concentric

CHAPTER 3

FIBER OPTIC DISPLACEMENT SENSOR WITH A REFLECTIVE TYPE

3.1 Introduction

Fiber optic displacement sensors will play an increasingly larger role in a broad range of industrial, military and medical applications [33]. Two particular advantages of fiber optic displacement sensors include the potential for extremely accurate non-contact sensing and the possibility of incorporating the optical sensors permanently in composite structures. Interest in the fiber-optic sensor is based on their inherent simplicity, small size, mobility, wide frequency capability, extremely low displacement detection limit and ability to perform non-contacting measurement. These properties have led to a variety of mechanical and biological measurement applications.

Multimode plastic fibers are in a great demand for the transmission and processing of optical signals in optical fiber communication system. They are also widely used in sensing applications because of their better signal coupling, large core radius, and high numerical aperture as well as able to receive the maximum reflected light from the target [34-35]. Some of the earliest absolute methods for displacement measurements are based on interferometric techniques [36-37].

In this chapter, a simple, rugged, low cost and very efficient fiber optic sensor is proposed for the measurement of displacements based on the intensity modulation technique. In this sensor the reflected light from mirror is coupled back into a fiber

from a reflecting surface and this power is compared with a portion of power emitted by the same light source.

3.2 Experimental Setup for the Reflective Type Displacement Sensor

The schematic diagram of the experimental set-up is shown in Fig. 3.1. It consists of a light source, a fiber optic probe and a silicon detector, which is connected to a lock-in amplifier and computer. The fiber probe is a bundled plastic fiber 2m long, which consists of one transmitting core and one or more receiving cores. The light source is a He-Ne laser with a peak wavelength of 633nm, which is modulated externally by chopper with a frequency of 200Hz. The modulated light source is used in conjunction with lock-in amplifier to reduce the dc drift and interference of ambient stray light. In this displacement sensor, the intensity modulation technique is adopted and a mirror is used as a reflecting target. The light from a light source enters a transmitting core and then radiates to the target, and the light reflected from object surface is transmitted through the receiving core to a photo-detector. The amount of light returning to detector depends on the displacement between the end of the probe and the target being monitored. For the displacement a flexible adjusting mechanism using piezoelectric is required.

The bending losses are minimized by putting both transmitting and receiving fibers in close contact, thus forming a curvature of equal radius. The experiment is carried out for three types of bundled fibers as discussed in the previous chapter. The optical fibers in the bundled front-end are arranged concentrically in both types B and C and as a pair in the bundled fiber type A. The transmitting core is surrounded by the receiving fibers in the concentric arrangement. In the pair arrangement, the transmitting and receiving fibers are placed side by side. Static displacement of the target is achieved

by mounting it on a translation stage. The distance between the fiber optic probe and the target is varied in successive steps of 25 µm. (in negative steps and maximum 50µm for positive steps, The signal from the detector is converted into a voltage and is measured using a computer automatically using Delphi software through serial port RS 232. The piezoelectric micrometer provides precise change of displacement in both positive and negative directions.

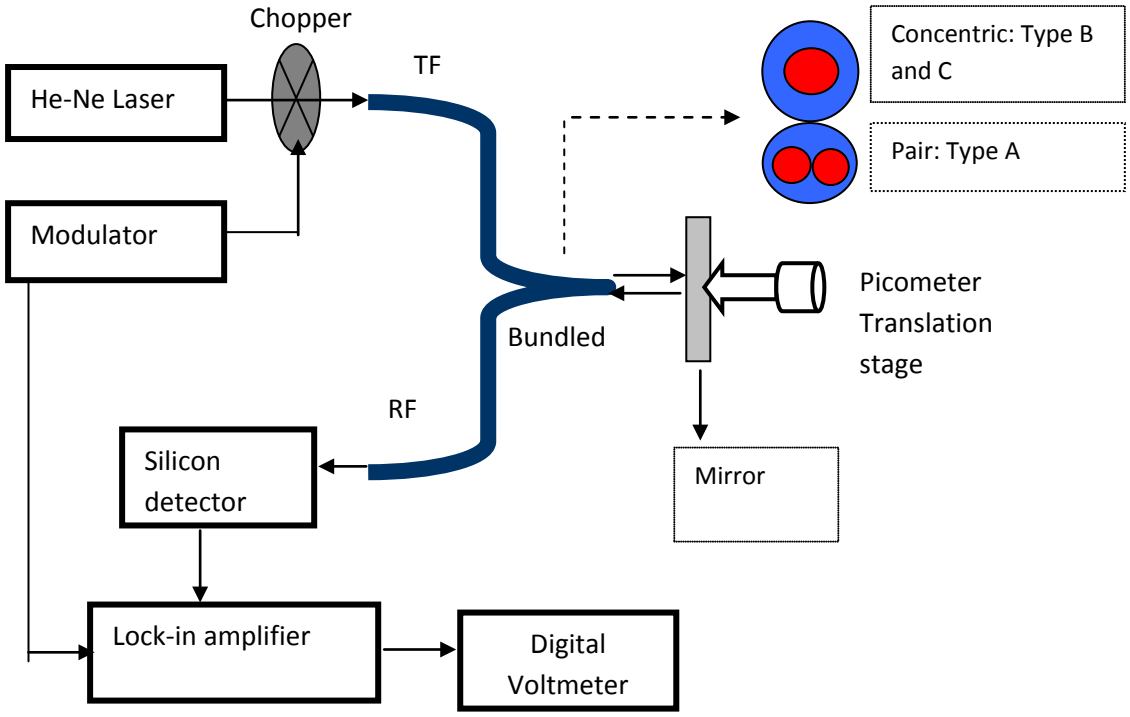

Fig. 3.1: Experiment setup of fiber optic displacement sensor. (TF: Transmitting fiber, RF: receiving fiber)

3.3 Comparing the Experimental Results with the Theoretical Results

The theoretical result in Eq. 2.13 of Chapter 2 is presented graphically and compared with an experimental result in Fig. 3.2 for a pair type of bundled fiber (Type A). The specification of the fiber has been described in Table 2.1 of the previous chapter. The plotted graph shows the normalized collected output power versus the normalized distance. Both curves exhibit a maximum with a steep front slope and back slope which follows an almost inverse square law relationship for the output power against a displacement distance. At h = 0, the plotted optical power does not equal to zero as expected. This is true for both the theoretical and experimental results, but more pronounced in the experimental results. This is due to the Gaussian beam truncation effect caused by the opaque outer jacket that covers the transmitting fiber and consequently prevents the light cone from reaching the receiving core. When the displacement is increased, the size of the reflected cone of light at the plane of the fiber increases and starts overlapping with the receiving cores, leading to a small output power. A further increase in the displacement leads to larger overlapping which results in a further increase in the output power. However, after reaching the saturation region, the output power starts decreasing for larger displacements. This is due to the large increase in the size of the light cone and the subsequent decrease in the power density. The maximum normalized output power is obtained at a displacement distance of 1050 μm and 1750 μm with the theoretical and experimental approaches respectively.

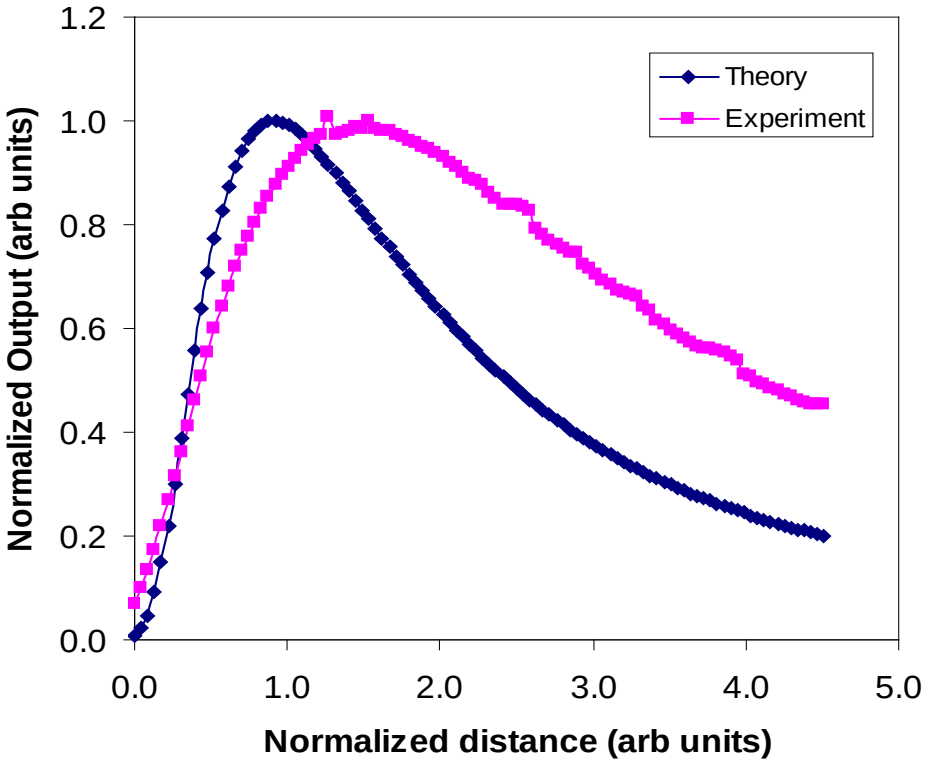

Fig. 3.2: Normalized Output versus normalized distance for Type A sensor.

Both the theoretical slope and experimental slope curves show a good linearity as shown in Fig. 3.3 with a certain regions exhibits linearity of more than 99%. For the front slopes, the high linearity areas are obtained at a normalized displacement of 0.13 ~ 0.61 (corresponding to a displacement of 150 -700 μm) for the theoretical approach and 0.09 ~ 0.79 (corresponding to a displacement 100-900 μm) for the experimental result. On the other hand, the back slopes show a high linearity in the range of 1.14 ~ 2.15 (corresponding to a displacement of 1300~2450 μm) for the theoretical results and 1.80 ~ 3.59 (correspond with normalized displacement of 2050~4100μm) for the experimental result. The sensitivity and linearity of both the front and back slopes of Figure 3.3 are summarized in Table 3.1. According to Eq. 2.15, zero sensitivity occurs

for $\zeta = \sqrt{8}$ when P_N reaches its peak. The sensitivity is positive on the front slope and negative on the back slope.

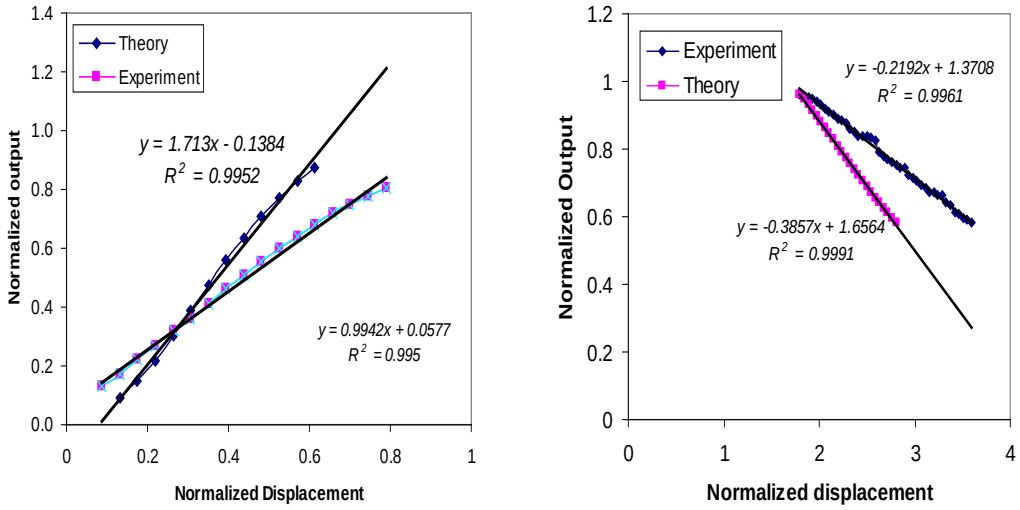

(a) (b)

Fig. 3.3: Linearity range and sensitivity of the sensor for (a) the front slope and (b) the back slope

Table 3.1: Comparison of the performance of the sensor with theoretical and experimental approaches

Methods	The front slope			The back slope		
	Sensi-tivity	Linearity range		Sensi-tivity	Linearity range	
		Norma-lized displa-cement, h_N	Displa-cement(μm)		Norma-lized displa-cement, h_N	Displa-cement (μm)
Theoreti-cal	1.7130	0.4821 (0.1314~ 0.6135)	550 (150~700)	0.3857	1.0080 (1.1394~ 2.1474)	1150 (1300~ 2450)
Experi-mental	0.9942	0.7012 (0.0876~0.7888)	800 (100~900)	0.2192	1.7968 (1.7968~ 3.5936	2050 (2050~ 4100)

The fiber bundled sensor shows a longer linear range of 800μm and 2050μm for both the front and back slopes respectively as determined experimentally with a lower sensitivity compared to theoretical value. On the front slope the sensitivities are obtained at 1.71 and 1.0 mW/μm for the theoretical and experimental approaches respectively, while on the back slope the sensitivities are 0.38 and 0.22 mW/μm for theoretical and experimental approaches respectively, which is smaller than the front slope. This discrepancy in theoretical and experimental values is due to neglecting the Gaussian beam truncation effects in our simple theoretical model. As indicated by the above results, we can conclude that the front slope is highly sensitive and useful for close distance targets while the back slope is less sensitive and useful for large

displacement movements. The experimental results are capable of offering quantitative guidance for the design and implementation of the displacement sensor.

3.4 Comparing the Performance of the Sensors between Positive and Negative Displacements.

This section compares the performance of the sensor using positive and negative movements of the mirror to investigate the repeatability. In the this experiment, the probe is set to be close to the target before it is moved away (negative displacement) or moved closer (positive displacement) from/to the mirror by the piezoelectric (in interval of 25µm). The type C of bundled fiber is used in this experiment. Fig. 3.4 shows output voltage curve against the displacement of mirror for different displacements direction (negative or positive). Both curves of positive or negative displacements show the similar pattern with two slopes. With the positive displacement, the sensor front slope sensitivity is obtained at 0.001mV/µm in the range of 150µm. The similar sensitivity and measure range are obtained for the negative displacement. The resolution which is defined as the smallest change it can detect in the quantity that it is measuring, is the almost same for both displacements around 10µm. For the back slopes, the sensitivities are obtained at 0.0002 mV/µm (within the range of 250µm) and 0.0003mV/µm (within the range of 250µm) for the positive and negative displacements, respectively. The resolution is almost same for both positive and negative displacements. This result shows that is no significant different between positive and negative or the repeatability of sensor is a very good.

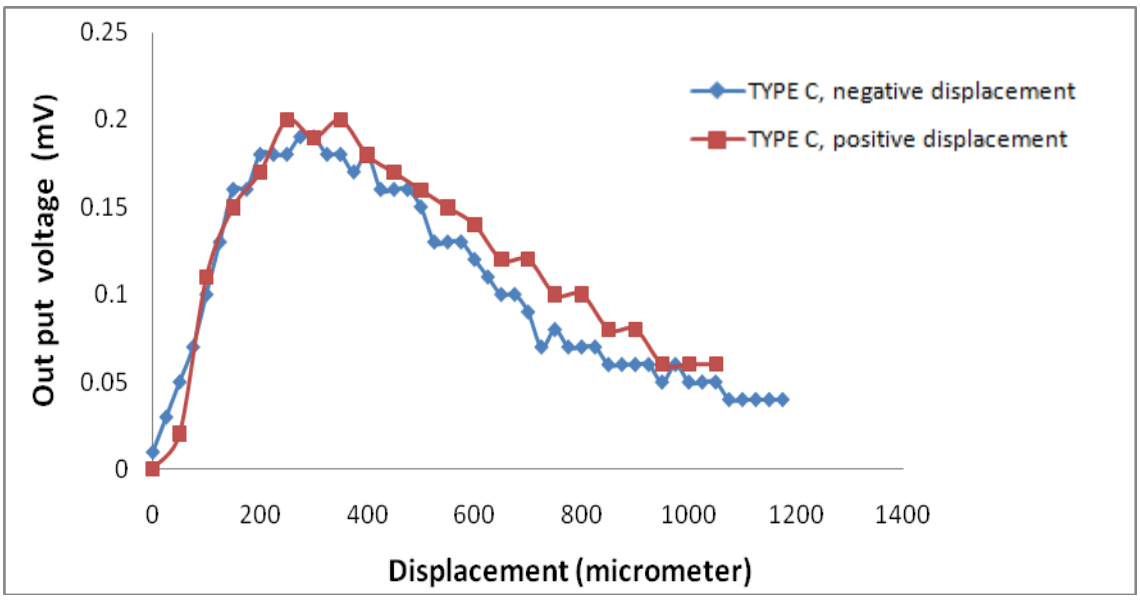

Fig. 3.4: Variation of the output for both positive and negative pulses with type C sensor.

3.5 Displacement Sensor Performance for Different Bundled Fiber Types

Fig. 3.5 shows the variation of the output voltage against the displacement of the mirror from the fiber optic probe using different bundled fibers types. The types of fibers are shown in Table 2.1 of the previous chapter. The experimental results are obtained using the positive pulse technique. The intensity of the detected light depends on the distance of the reflecting target or mirror from the fiber probe. All the curves exhibit a maximum with a steep linear front slope and back slope which follows an almost inverse square law relationship for the reflected light intensity versus distance of the mirror from fiber optic probe. The signal is minimal at zero distance because the light cone does not reach the receiving cores. When the displacement is increased, the size of the reflected cone of light at the plane of fiber increases and starts overlapping with the receiving cores leading to a small output voltage. Further increase in the displacement leads to large overlapping which results in increase in output voltage. However, after reaching the maximum value, the output voltage starts decreasing as the

displacement increases. This is due to the large increase in the size of the light cone and the power density decreases with the increase in the size of the cone of light. The maximum output voltage obtained are 0.20 (arb.units) for a distance of 1140 μm (type A), 0.26 (arb.units) for a distance of 510 μm (type B), 0.23 (arb.units) for a distance of 350 μm (type C) between the mirror and the fiber-optic probe.

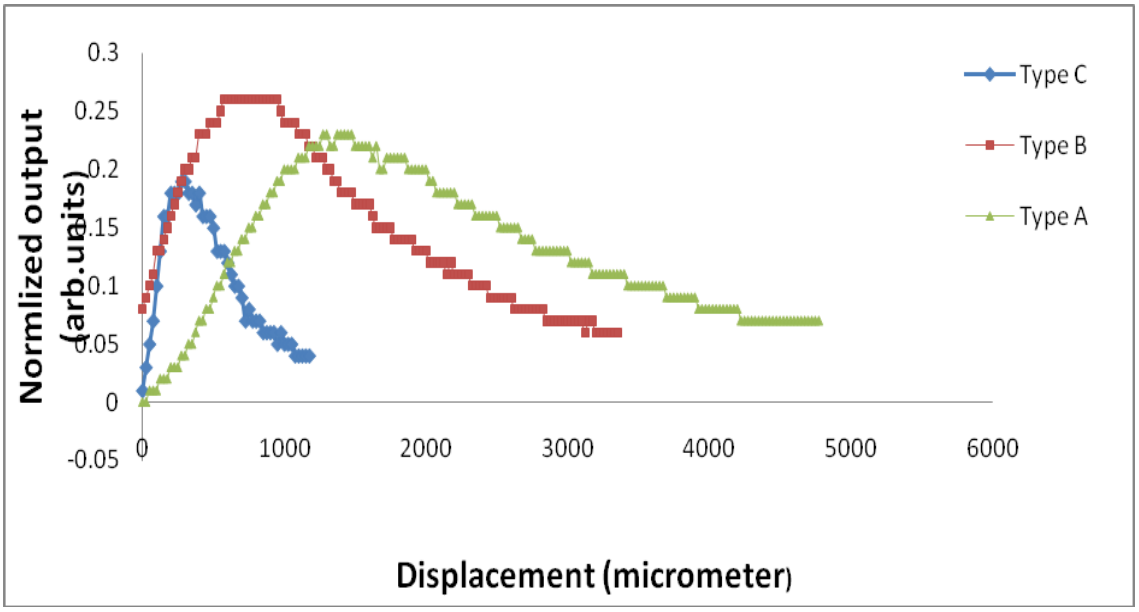

Figure 3.5: Variation of the output voltage with the displacement of the mirror from the fiber-optic probe.

Both slopes show a good linearity as shown in Fig. 3.5 with a certain regions exhibits linearity of more than 99%. For the front slopes, the high linearity ranges are obtained at 150-1000 μm, 0-400 μm, and 100-450 μm for type A, B and C respectively. On the other hand, the back slopes show a high linearity in the range of 150-810 μm, 0-390 μm, and 50-200 μm for type A, B and C, respectively. The sensitivity and linearity of both front and back slopes of Fig. 3.5 are summarized in table 3.2. Type A of the fiber bundle sensor shows the longest linear range of 660 μm and 1080 μm for both the

front and back slopes respectively, however it has the lowest sensitivity among the bundled fibers. The highest sensitivity of front and back slopes is obtained at 0.001 and 0.0002 mV/μm respectively with the type C bundled fiber. Type A shows the highest linearity range because it has the biggest receiving core diameter and is able to collect more reflected light compared to other types of fiber. The increase in the number of receiving cores as in type C increases the sensitivity of the sensor.

Table 3.2: Summary of the sensor performance with different bundled fibers used

No, of core	**Type of bundle fiber**	**Sensitivity of front slope (mV/μm)**	**Linearity range of front slope (μm)**	**Resolution**	**Sensitivity of back slope (mV/μm)**	**Linearity range of back slope (μm)**	**Resolution**
1	Type A	0.0002	660 (150-810)	50	-7e-5	1080 (2040-3120)	142
9	Type B	0.0005	390 (0-390)	20	-0.0002	930 (750-1680)	50
16	Type C	0.001	150 (50-200)	10	-0.0002	250 (650-400)	50

3.6 Displacement Sensor Performance Using a Real Object as the Target

This section demonstrates a simple fiber optic displacement sensor using the intensity modulation technique to measure a displacement from a probe and real object as the target. The sensor uses a multimode plastic bundled fiber as a probe and red He-Ne laser as a source. The sensitivity and linearity range of the sensor are investigated for different types of real object as a target. The performance of the sensor is also

investigated for different types of bundled fiber as shown in Table 2.1 of the previous chapter.

Fig. 3.6 shows the variation of the output voltage against the displacement of the target from the fiber optic probe using different bundled fibers types. The stainless steel block which has a reflectivity of approximately 74% is used as a reflecting target. The intensity of the detected light depends on the distance of the target from the fiber probe. All the curves exhibit the same pattern with two slopes as the previous experiments. The maximum output voltage obtained are 14.2 mV for a distance of 800 μm (type C), 8.9 mV for a distance of 750 μm (type B), 7.3 mV for a distance of 1500 μm (type A) between the stainless steel block and the fiber-optic probe.

Both front and back slopes show a good linearity as shown in Fig. 3.6 with certain regions exhibiting a linearity of more than 99%. For the front slopes, the high linearity ranges are obtained at 150-550 μm, 50-450 μm, and 50-900 μm for Type C, B and A respectively. On the other hand, the back slopes show high linearity in the range of 1100-2000 μm, 1100-2000 μm, and 1900-4000 μm for the Type C, B and A bundled fibers, respectively. The sensitivity and linearity of both front and back slopes of Fig. 3.6 are summarized in Table 3.3. The Type A fiber sensor shows the longest linear range of 850 μm and 2000 μm for both the front and back slopes respectively, however it also has the lowest sensitivity among the bundled fibers. The highest sensitivity of front and back slopes is obtained at 0.0220 and 0.0061 mV/μm respectively with the Type C bundled fiber. The Type A sensor shows the highest linearity range because it has the largest receiving fiber diameter and is able to collect more reflected light as compared to the other fiber sensor types. The increase in the number of receiving fibers as in the Type C sensor increases the sensitivity of the sensor.

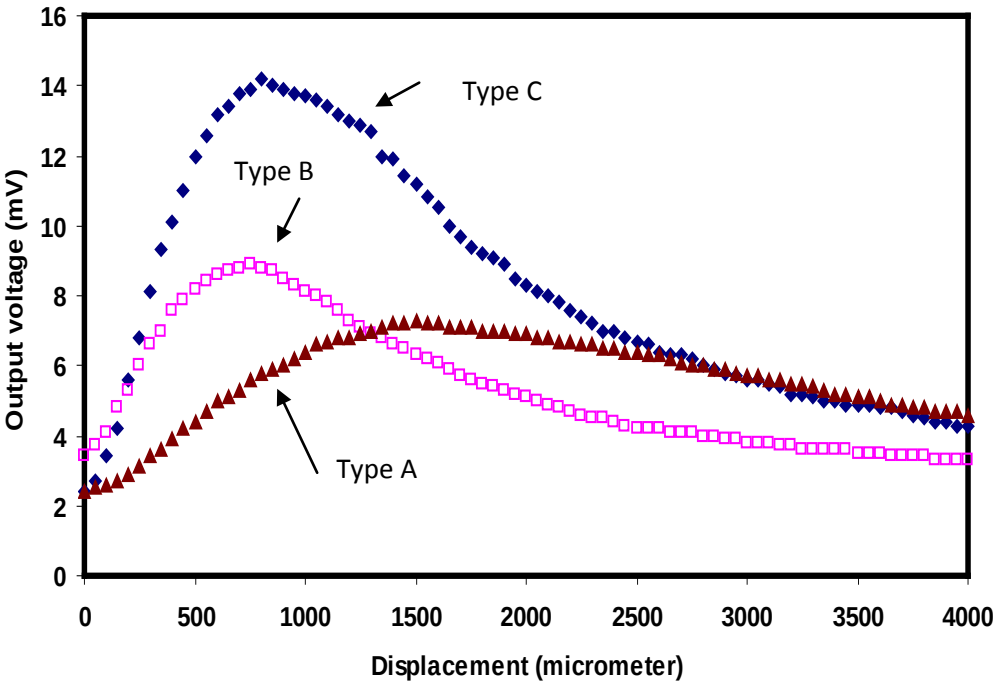

Fig. 3.6: Variation of the output voltage with the displacement of the stainless steel block from the fiber-optic probe.

Table 3.3: Performance of the sensor at different type of fiber bundle

	Type of bundle fiber	Sensitivity of front slope (mV/μm)	Linearity range of front slope (μm)	Sensitivity of back slope (mV/μm)	Linearity range of back slope (μm)
1	Type C	0.0220	400	-0.0061	900
2	Type B	0.0104	400	-0.0029	900
3	Type A	0.0044	850	-0.0012	2100

Fig. 3.7 shows the variation of the output voltage with the displacement of the target for various target's materials. The target is a flat mirror or a flat surface object which made from different type of materials such as stainless steel, aluminium, copper and plastic. The reflectivity of the mirror, stainless steel, aluminium, copper and plastic objects are measured to be 100, 74, 70, 62 and 30%, respectively by comparing the powers of the light source before and after reflecting object. The bundled fiber used in the experiment is Type C with 16 receiving fibers for better sensitivity. All curves show a similar pattern with two slopes. As shown in figure 3.7, the voltage obtained increases with the reflectivity of the target. The maximum peak voltage is obtained at 31.8 mV for the mirror and the minimum peak voltage is obtained at 5.2 mV for the plastic. The sensitivity and linearity range of the sensor is summarized in Table 3.4. The highest and lowest sensitivities are obtained using the mirror and plastic target respectively. Higher reflectivity objects show a higher sensitivity, while the linearity range for front slope is almost similar for all materials, which varies from 350 to 450 μm. However, for the back slope, the lower reflectivity object relatively has a higher linearity range with the highest range of 1600 μm being obtained with plastic and aluminium objects. This is attributed to the lower reflectivity objects reflect lower power. The slope is relatively shallower at small powers, which contributes to a larger linearity range. In these displacement sensors, the front slope is highly sensitive and useful for close distance target and the back slope is less sensitive and useful for long distance measurement. The experimental results are capable of offering quantitative guidance for the design and implementation of the displacement sensor. This sensor has many potential applications in various industries such as automated monitoring control, position control and micro-displacement sensor in the hazardous regions.

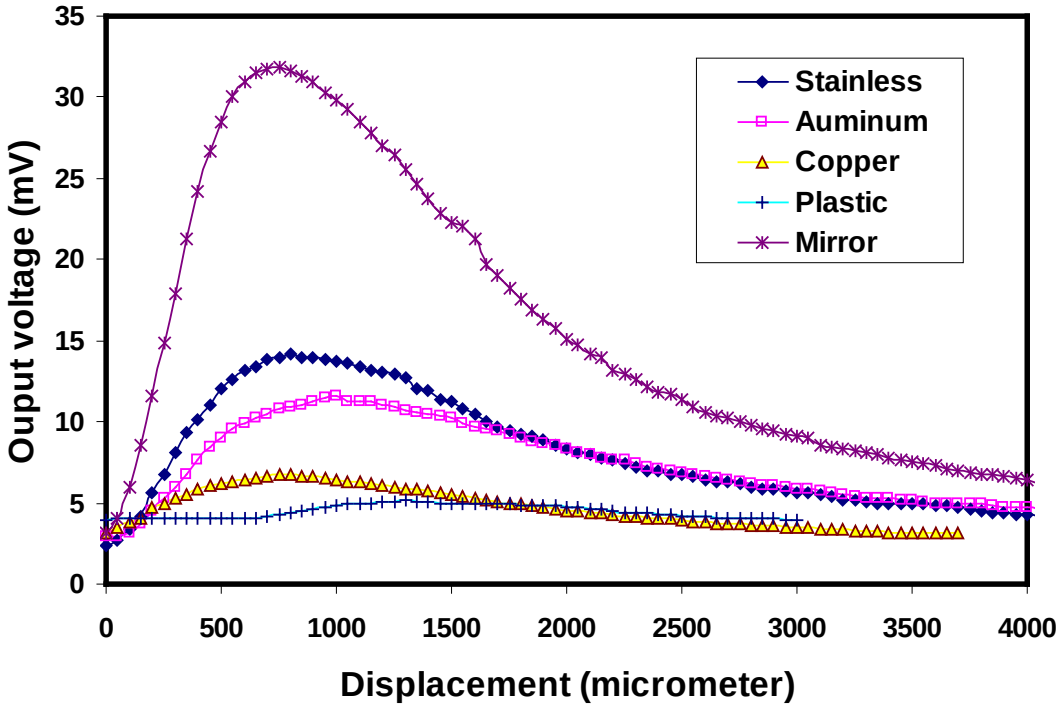

Fig. 3.7 Output voltage against object displacement for various objects.

Table 3.4: The performance of the bundled sensor at different objects

Object	The front slope		The back slope	
	Sensitivity (mV/μm)	Linearity range (μm)	Sensitivity (mV/μm)	Linearity range (μm)
Stainless Steel	0.0220	400 (150 ~ 550)	0.0061	900 (1100 ~2000)
Aluminium	0.0150	350 (150 ~500)	0.0032	1600 (1200 ~2800)
Copper	0.0066	400 (50 ~ 450)	0.0017	1450 (1100 ~ 2550)
Plastic	0.0020	450 (650 ~ 1100)	0.0008	1600 (1400 ~ 3000)
Mirror	0.0562	450 (100 ~ 550)	0.0151	1050 (950 ~ 2000)

In summary, a simple fiber optic displacement sensor is presented using a multimode plastic bundled fiber and the intensity modulation technique. The

performance of the sensor is compared for different types of probes and targets. The probe with the largest receiving core diameter demonstrates the highest linearity range, and increasing the number of receiving cores increases the sensitivity of the sensor. With a stainless steel target and the concentric bundled fiber with 16 receiving fibers as a probe, the sensitivity of the sensor is found to be 0.0220 mV/μm over 150 to 550 μm range and -0.0061 mV/μm over 1100 to 2000 μm range. The target with a higher reflectivity shows a higher sensitivity. The linearity range for the front slope is almost similar for all targets tested. However, for the back slope, lower reflectivity objects have a relatively higher linearity range with the highest range of 1600 μm being obtained using plastic and aluminium targets. The simplicity of the design, high degree of sensitivity, dynamic range, non-contact measurement and low cost of the fabrication

CHAPTER 4

LATERAL AND AXAIL DISPLACEMENTS MEASUREMENTS BASED ON BEAM-THROUGH METHOD

4.1 Introduction

Fibre optic technology offers the possibility for developing of a variety of physical sensors for a wide range of physical parameters. The use of bundle fibers for sensor applications allows us to obtain very high performances in their response to many physical parameters (displacement, pressure, temperature, electric field etc.) compared to conventional transducers. The intensity modulation is the simplest technique for a displacement measurement. It is based on comparing the transmitted light intensity against that of the launch light which can provide information on the displacement between the probe and the target. This chapter presents a rather simple design for an intensity-based displacement sensor using a multimode plastic fiber in conjunction of through beam method. The performances of this sensor are investigated for both lateral and axial displacements. In the sensor, light is transmitted through a transmitting fiber to a receiving fiber and the received light is finally measured by a silicon detector.

4.2 Experimental Setup

Fig 4.1 shows a schematic diagram for the axial and lateral displacements measurement. The sensor uses a beam-through technique, which consists of two set of

fiber, one set is connected to a light source and is termed as the transmitting fiber, and the other set is connected to a silicon detector and is known as the receiving fiber. In the experiment, the transmitting fiber located opposite to the receiving fiber is moved laterally and axially as shown in Fig.4.1. The light is scattered after travelling out from the transmitting fiber and the receiving fiber collect a portion of the scattered light to transmit into the silicon detector where its intensity is measured. The intensity of the collected light is a function of axial and lateral displacement of the fiber.

The light source is a He-Ne laser with a peak wavelength of 633nm, which is modulated externally by chopper with a frequency of 200Hz. The modulated light source is used in conjunction with lock-in amplifier to reduce the dc drift and interference of ambient stray light. For an axial and lateral displacement, a flexible adjusting mechanism using piezoelectric is required, so the receiving fiber tip is mounted on a translational stage, which provides fine movement of the transmitting fiber surface in the axial and lateral direction. In this experiment, the axial and lateral micro-distance is varied and the lock-in amplifier output voltage of the transmitted light is directly recorded by a computer automatically using Delphi software through serial port RS232. The piezoelectric micrometer can provide precise changes of about 25nm and 30nm for every positive and negative pulse, respectively and in this experiment the displacement measurement is taken in successive steps of 45μm.

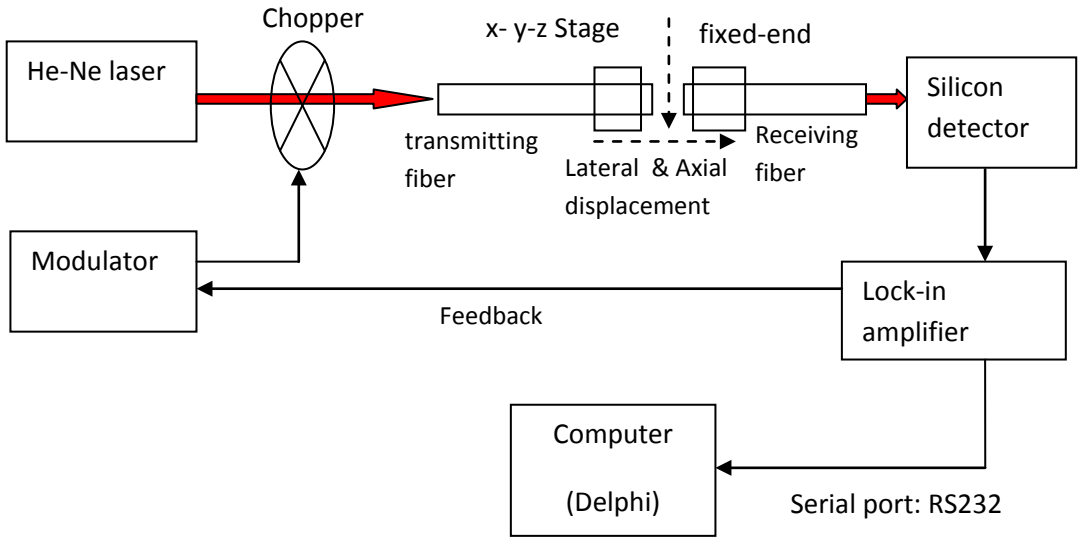

Fig 4.1: Schematic diagram for the fiber-optic displacement sensors.

4.3 Result and Discussion

The output voltage from a receiving fiber is related to the axial and lateral displacements of the transmitting fiber. Both fibers should be mounted perpendicular to each other and positioned flush against the surface. The output voltage of the sensor should be highest in this position. The transmitting fiber is then moved away laterally and axially from the receiving fiber tip by still maintaining perpendicularity between them. Fig. 4.2 shows the output voltage of the lock-in amplifier against the lateral displacement between the two ends of the fibers. In the experiment the core diameter for both ends are varied. As expected, the voltage is highest at zero displacement from the center and the lateral movements of the transmitting fiber away from the receiving fiber resulted in a reduced output voltage as shown in the figure. The power drop pattern

follows the theoretical analysis by Van Etten and Van der Plaats. [38], which the output transmission function is given by:

$$\eta = \frac{2}{\pi}\left(\left(\arccos\left(\frac{d}{a}\right) - \frac{d}{a}\sqrt{1-\left(\frac{d}{a}\right)^2}\right)\right) \qquad \text{(Eq.4. 1)}$$

where η, d and a is coupling efficiency, lateral displacement and fiber core radius, respectively. η is defined as the ratio of output voltage over the maximum voltage.

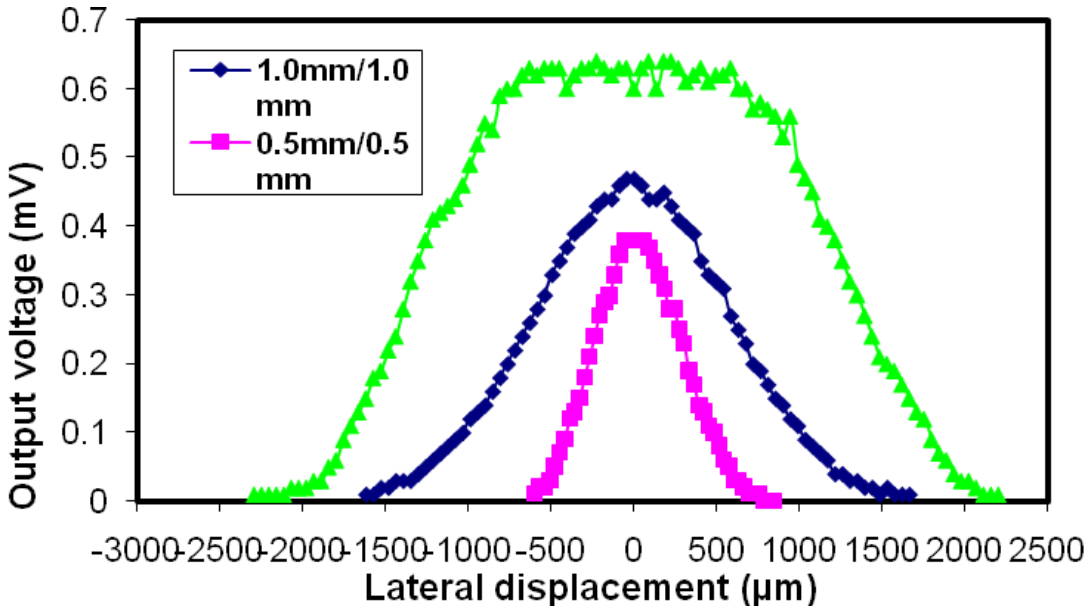

Fig.4.2: The output voltage of the lock-in amplifier against the lateral displacement of the transmitting fiber.

The sensitivity of the sensor is determined by a slope of a straight-line portion in the curves. As shown in Fig 4.2, the beam-through type of sensor has two symmetrical slopes and the sensitivity is higher at the smaller core diameter. At core diameter of 0.5mm for both transmitting and receiving fibers, the sensitivity is obtained at around 0.0008mV/µm and the slope shows a good linearity of more than 99% within a range of

420 μm. The linear range increases to around 800 μm for the both slopes as the core diameter increased to 1.0mm. The linear range can be further increased to more than 1000 μm by using a larger core for the receiving fiber as shown in Fig. 4.2. However, the voltage is unchanged at a small lateral displacement for this sensor due to the larger receiving core, which covers the whole diverged beam from the transmitting fiber. The highest resolution of approximately 13μm is obtained with core diameter of 0.5mm for both fibers. In this work, the resolution is defined as the minimum displacement which can be detected by this sensor. The performance of the sensor with lateral displacement is summarized as shown in Table 4.1.

Table 4.1: Performance of the lateral displacement sensor

Fiber's core diameter	The left slope		The right slope		Resolution (μm)
	Sensitivity (mV/μm)	Linear range (μm)	Sensitivity (mV/μm)	Linear range (μm)	
1.0mm/1.0mm	0.0003	855 (585-1440)	0.0004	765 (1845-2610)	33
0.5mm/0.5mm	0.0008	420 (120-540)	0.0007	420 (750-1170)	13
0.5mm/1.0mm	0.0005	1035 (450-1485)	0.0005	1125 (3060-4185)	20

The output voltage from a receiving fiber is related to axial displacement of end surface of the transmitting fiber. Fig. 4.3 shows the output voltage of the lock-in amplifier against the axial displacement for the different core diameters. In this experiment, the end surface of transmitting fiber is moved away from the receiving fiber tip by still maintaining perpendicularity between them.

As expected, the voltage is highest at zero displacement from the center and the output voltage reduces as the axial displacement increases for all core diameters used. The power drop pattern follows the theoretical analysis by Van Etten and Van der Plaats. [38], which the output transmission function is given by:

$$\eta \approx 1 - \frac{z}{a}\frac{2}{\pi (NA)^2}\left[\arcsin(NA) - NA\sqrt{1-(NA)^2}\right] \qquad \text{(Eq.4.2)}$$

where η, z, a and NA is coupling efficiency, axial displacement, core radius, and numerical aperture, respectively.

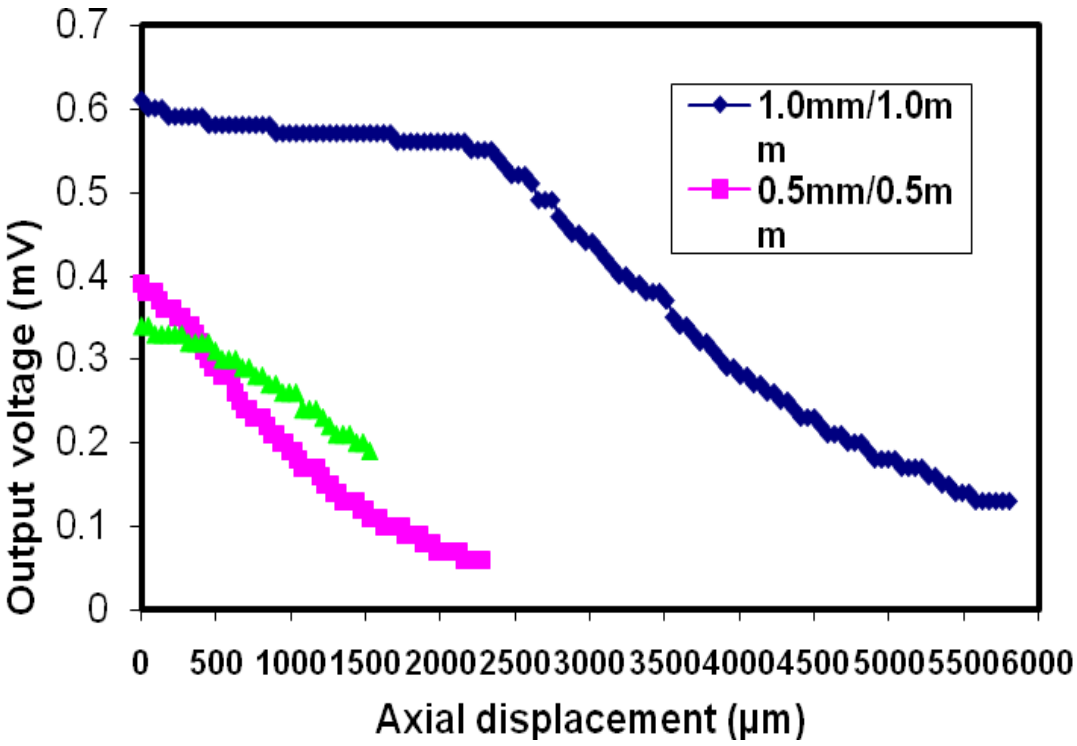

Fig.4.3: The output voltage of the lock-in amplifier against the axial displacement of the transmitting fiber.

As shown in Fig 4.3, the sensors only have one slope and the sensitivity is higher at the smaller core diameter. At core diameter of 0.5mm (for both transmitting and receiving fibers), the sensitivity is obtained at around 0.0002mV/μm, which is the highest and the slope shows a good linearity of more than 99% within a range of 900 μm. The linear range increases to 3195 μm with the larger core diameter of 1.0mm. In case of the receiving core is bigger than the transmitting core, the voltage is almost constant at small axial displacements due to the coherent light source, which has a small divergence angle. The highest resolution is obtained at approximately 50μm with 0.5mm core diameter for both fibers.

The performance of the sensors with axial displacement is summarized as shown in Table 4.2. The stability of these sensors are observed to be less than 0.01mV (3%). The experimental results are capable of offering quantitative guidance for the design and implementation of the displacement sensor. This sensor has many potential applications in various industries such as automated monitoring control, position control and micro-displacement sensor in the hazardous regions.

Table 4.2: Performance of the axial displacement sensor

Fiber's core diameter	Sensitivity (mV/μm)	Linear range (μm)	Resolution (μm)
1.0mm/1.0mm	0.0001	3195 (2340-5535)	100
0.5mm/0.5mm	0.0002	900 (0-900)	50
0.5mm/ 1.0mm	0.0001	1530 (0-1530)	100

CHAPTER 5

CONCLUSION AND SUGGESTION FOR FUTURE WORK

5.1 Conclusion

Fiber optic sensors are becoming an important field that attracted many applications in various fields. One of the applications of the sensor is in a high-precision non-contact displacement measurement, which is the key to micro-nano technologies. In a displacement sensor, two methods are commonly adopted, namely laser interferometry and intensity modulation techniques. Laser interferometry which is based on the fringe counting method has high resolution and stability, but its precision and stability is dependent on the wavelength of light. Comparatively, the intensity modulation technique is a significantly simpler method for non-contact displacement measurements while at the same time being able to provide high resolutions. The intensity modulation technique uses either reflective or beam through (transmittive) technique for light detection. In the reflective type of sensor the reflected light from the mirror is coupled back into a fiber from a reflecting surface and this power is compared to a portion of the power emitted by the same light source. The beam-through type is based on comparing the transmitted light intensity against that of the launch light which can provide information on the displacement between the probe and the target. The interest in the intensity-modulation type of displacement sensors is based on its inherent simplicity, small size, mobility, wide frequency capability, extremely low displacement detection limit and ability to perform non-contact measurements. These properties have led to a variety of applications, not only as a displacement or vibration sensor, but also as a secondary transducer for measuring physical properties that correlate to the amount of displacement such as temperature, pressure and sound.

Multimode plastic fibers are in a great demand for the transmission and processing of optical signals in optical fiber communication system. They are also widely used in sensing applications because they provide better signal coupling, have a large core radius and high numerical aperture as well as able to receive the maximum reflected light from the target. In this study, both reflective and beam-through types of fiber optic displacement sensors are proposed using the multimode bundled fiber to measure a displacement. The sensor uses a He-Ne laser, which is externally modulated as a source. The sensitivity and linearity range of the sensor are investigated for different types of real object as a target. The performance of the sensor is also investigated for different types of bundled fibers.

Firstly, we investigated the performance of an optical displacement sensor using a pair type bundled fiber from both the theoretical and experiment perspectives. The theoretical analysis uses an electromagnetic Gaussian beam approach to determine a transfer function of the sensor. The displacement between a flat mirror and the bundled fiber end is measured using an intensity modulation technique. The sensor has two operating ranges with a good linearity; namely the front slope and back slope. On the front slope the sensitivities are obtained at 1.71 and 1.0 mW/μm for the theoretical and experimental approaches respectively while on the back slope the sensitivities are 0.38 and 0.22 mW/μm for theoretical and experimental approaches respectively. This discrepancy in theoretical and experimental values is due to neglecting the effect of Gaussian beam truncation in our simple theoretical model. The front slope is highly sensitive and useful for close distance targets while the back slope is less sensitive and useful for large displacement movements.

The second part of this study demonstrated a simple and effective fiber optic micro displacement sensor based on the reflective technique. The sensor uses a bundled multimode fiber designated as types A, B and C as a fiber-optic probe, a red laser with peak wavelengths of 633 nm as a light source and lock-in amplifier system to reduce the dc drift and interference of ambient stray light. The type C bundled multimode fiber sensor has the highest sensitivity because it has the highest number of receiving cores. Type A has the highest linearity range because it has the biggest receiving core diameter. The experimental results also show that the sensor is more sensitive with higher reflectivity object as a target. With the stainless steel as a target and the concentric bundled fiber with 16 receiving fibers as a probe, the sensitivity of the sensor is found to be 0.0220 mV/μm over 150 to 550 μm range and -0.0061 mV/μm over 1100 to 2000 μm range. The linearity range for front slope is almost similar for all targets tested. However, for the back slope, the lower reflectivity object relatively has a higher linearity range with the highest range of 1600 μm being obtained with plastic and aluminum objects. The simplicity of the design, high degree of sensitivity, dynamic range, non-contact measurement and low cost of the fabrication make it suitable for applications in industries for position control and micro displacement measurement in the hazardous regions.

Finally, the performance of the fiber-optic displacement sensor with beam-through detection technique has been demonstrated. The effects of lateral and axial displacements on the detected output voltage are investigated. The highest sensitivity is obtained at 0.0008mV/μm for the lateral displacement with core's diameters for both transmitting and receiving fibers are fixed at 0.5mm. The widest linear range is obtained at 3195μm for the axial displacement with 1.0 mm core's diameters for both fibers. The sensor with the smaller core normally shows a better sensitivity with the expense of the

smaller linear range. The sensor with the smaller core also exhibits a better resolution. The highest resolution of the 13μm is obtained with the lateral displacement sensor with 0.5mm core diameter.

5.2 Future Work

Future work should be focused on the use of optical fiber displacement sensor for the measurement of amplitude and frequency of vibration. Considering its advantages of simplicity, long term stability, low power consumption, wide dynamic and frequency ranges, linearity, noise reduction, ruggedness and light weight of the reflective surface mounted on the mini-shaker, this fibre optic sensor is a promising alternative to other well-established methods for the measurement of amplitude and frequency of vibration. The sensor applications include monitoring of commercial machinery, airframes, turbines and helicopter gearboxes and civil structures. The ability of the fibre optic sensor to work close to the reflecting surface without the need for special optics is especially advantageous for embedded sensor applications. The stable sensor is ideal for use as an embedded sensor, requiring minimal maintenance even in relatively harsh environments. Apart from the vibration sensor system, the fibre optic probe has applications in various industries, radar systems and in aircraft flight control systems. With the emerging fly-by light concept, the fibre optic probe solves many sensing problems in aircraft. Moreover, accuracy and reliability are the excellent pay-offs of this fibre optic sensor.

References

1. P. M. Sandeep, S.W. B. Rajeev, M. Sheeba, S. G. Bhat, and V. P. N. Nampoori, “Laser induced fluorescence based optical fiber probe for analyzing bacteria,” Laser Phys. Lett. 4 , 611–615 (2007).
2. M. V. Alfimov and A. M. Zheltikov, “The figure of merit of a photonic-crystal fiber beam delivery and response-signal collection for nanoparticle-assisted sensor arrays,” Laser Phys. Lett. 4 , 363– 367 (2007).
3. A. Bergamin, G. Cavagnero, and G. Mana, “A displacement and angle interferometer with subatomic resolution,” Rev. Sci. Instrum., 64, 3076–3081 (1993).
4. Y. Zhao, M. Rong and Y. Liao, Reflex optical fiber sensor and compensation technique for temperature measurement under offshore oil well, *Chin. J. Lasers* **30** (2003), pp. 75–78.
5. J. Park, M. Kim, Y. Kim, K. Kim and I. Kim, Intensity-based fiber optic pressure sensor with an Au/NiCr/Si_3N_4/$Si0_2$/Si_3N_4 diaphragm, *Proc. SPIE* **3897** (1999), pp. 565–569.
6. G. He and F.W. Cuomo, Displacement response detection limit and dynamic range of fiber-optic lever sensors, *J. Lightwave Technol.* **9** (1991), pp. 1618–1625.
7. S. Nalwa (ed.), Polymer Optical Fibers (American Scientific Publishers, California, 2004).
8. Tyndall, John (1870). "Total Reflexion". *Notes about Light*.
9. Hecht, Jeff (1999). *City of Light, The Story of Fiber Optics*. New York: Oxford University Press.

10. Bates, Regis J (2001). *Optical Switching and Networking Handbook*. New York: McGraw-Hill.
11. Nishizawa, Jun-ichi; Suto, Ken (2004). "Terahertz wave generation and light amplification using Raman effect". in Bhat, K. N.; DasGupta, Amitava. *Physics of semiconductor devices*. New Delhi, India: Narosa Publishing House. p. 27.
12. R.J. Mears, L. Reekie, I.M. Jauncey and D. N. Payne: “Low-noise Erbium-doped fibre amplifier at 1.54pm”, Electron. Lett., 1987, 23, pp.1026-1028
13. E. Desurvire, J. Simpson, and P.C. Becker, High-gain erbium-doped traveling-wave fiber amplifier," Optics Letters, vol. 12, No. 11, 1987, pp. 888-890
14. Russell, Philip (2003). "Photonic Crystal Fibers". *Science* **299** (5605): 358.
15. A.L.Harmer ”optical fiber sensor “.VTT Symposion ,No. 46,5-76(1984).
16. Byoungho Lee, “Review of the present status of optical fiber sensor” Journal of optical fiber Technology , Vol.9, pp.57_79 ,2003.
17. Bahareh Gholamzadeh, and Hooman Nabovati, “fiber optical sensor” Proceeding of World Academy Of Science ,Engineering and Technology, Volume 32 pp.2070-3740 ,2008.
18. K.T.V Grattan, B.T. Meggitt , “Optical fiber sensor technology “ pp . 4-5. Springer 1998.ch 1.
19. D. Akin Dakin and B. Culshaw, optical fiber sensor –principle and component . Vol.I ,Artech House , Boston.
20. F.Yu,S Yin, Fibr optic sensor ,Marcel-Dekker,2002
21. A. Weinert, Plastic Optical Fibers: Principles, Compounds, Installation, Wiley-VCH, Weinheim, 1999.
22. Hecht, J,” Understanding Fiber Optics” ,2nd edition , Sams Publishing 1993.

23. Jeunhomme, Luc B ," Single-Mode Fiber Optics: Principle and Application" ,Marcel Dekker,Inc, New York, 1983.
24. Aggarwal ,D. I shwar ," Optical Waveguide Manufacturing ", Fiber Optic , Editor, James C.Daly, CRC Press,Florida,1984.
25. E. Udd, Editor, *Fiber Optic Sensors: An Introduction for Engineers and Scientists*, Wiley, New York, 1991.
26. J. Dakin and B. Culshaw,*Optical Fiber Sensors: Principals and Components*, Volume 1, Artech, Boston, 1988.
27. B. Culshaw and J. Dakin, *Optical Fiber Sensors: Systems and Applications*, Volume 2, Artech, Norwood, 1989.
28. T. G. Giallorenzi, J. A. Bucaro, A. Dandridge, G. H. Sigel, Jr., J. H. Cole, S. C. Rashleigh, and R. G. Priest, "Optical Fiber Sensor Technology", IEEE J. Quant. Elec., QE-18, p. 626, 1982.
29. D. A. Krohn, *Fiber Optic Sensors: Fundamental and Applications*, Instrument Society of America, Research Triangle Park, North Carolina, 1988.
30. B. Chulsaw and J. Dakin, Optical Fiber Sensors-System and Application, Norwod, MA: Artech, 1989.
31. P. LoPresti and W. Finn, Fiber Optic System for Rapid Positioning of a Microelectronic Array, Applied Optics, Vol. 37, pp. 3426-3431, 1998.
32. J.B. Faria, A Theoretical Analysis of the Bifurcated Fiber Bundle Displacement Sensor, IEEE Trans. On Inst. And Meas., Vol. 47, No. 3, 1998.
33. R. C. Spooncer, C. Butler, B. E. Jones, "Optical fibre displacement sensors for process and manufacturing applications," Opt Eng, vol. 31, pp. 1632-1637, 1992.
34. S. Nalwa, Polymer optical fibres. California: American Scientific Publishers; 2004.

35. Vijay K. Kulkarini, Anandkumar S. Lalasangi, I.I. Pattanashetti, U.S. Raikar, ”Fiber-optic micro-displacement sensor using coupler”, Journal of Optoelectronics and Advanced Materials, vol. 8, pp. 1610-1612, 2006.
36. A. M. Murphy, M. F. Gunther, A. M. Vengsarkar, O. R. Claus, “Quadrature phase-shifted extrinsic Fabry-Perot optical fiber sensor,” Optic Letters, vol. 16, pp. 273, 1991.
37. A. Bergamin, G. Cavagnero, G. Mana, “A displacement and angle interferometer with subatomic resolution,” Rev. Sci. Instrum., vol. 64, pp. 3076-3081, 1993.
38. W. Van Etten and J. Van der Plaats, “Fundamentals of optical fiber communications”, Prentice-Hall, London, 1991